High Temperature. Vol. 43, No. 2, 2005, pp. 266–309. Translated from Teplofizika Vysokikh Temperatur, Vol. 43, No. 2, 2005, pp. 274–316.
Original Russian Text Copyright © 2005 by Yu. A. Neruchev, M. F. Bolotnikov, and V. V. Zotov.

REVIEW

Investigation of Ultrasonic Velocity in Organic Liquids on the Saturation Curve

Yu. A. Neruchev, M. F. Bolotnikov, and V. V. Zotov
Kursk State University, Kursk, 305000 Russia

Received October 7, 2003

Abstract—This review deals with the investigation of the ultrasonic velocity in organic liquids on the saturation curve and with analysis of the results obtained at the Kursk State University – KGU (before that, Kursk State Pedagogical Institute – KGPI) during the period from 1969 to the present day. Much attention is given to the description of the procedure of measurement of the sound velocity by the pulse-phase method developed at the Laboratory of Molecular Acoustics of the KGU and to the estimation of measurement errors. The data on the sound velocity along the saturation curve in a wide temperature range for three classes of organic liquids (saturated hydrocarbons, aliphatic alcohols, and aromatic hydrocarbons) are given in the form of tables. Characteristic features of the behavior of the sound velocity and adiabatic compressibility of liquid in the vicinity of the critical point are investigated, and the possibility of using the acoustic data for the calculation of the thermodynamic properties of liquids is studied.

1. INTRODUCTION

Present-day science and industry place heavy demands on the reliability of experimental data required for the calculation of the physicochemical properties of materials used as heat-transfer agents and refrigerants in power plants and chemical-engineering processes. A significant rise was observed in recent years of the activities aimed at developing data bases for the thermal properties of various materials (TRC, Scientific & Technical Information Network, NIST WEBBOOK, IVTANTERMO, ORGANIKA, etc.). In addition to the density, saturated vapor pressure, and isobaric heat capacity, the sound velocity is an important parameter employed in the calculations of the thermodynamic properties of matter.

The propagation of sound in real liquids is accompanied by irreversible loss of energy resulting in the absorption of sound by the medium. The irreversibility of the process of propagation of sound waves in a liquid is associated primarily with its viscosity and thermal conductivity. In addition, the inability of liquid to instantaneously return to the state of equilibri-

0018-151X/05/4302-0266

um after being disturbed by a sound wave likewise results in deviations from the adiabaticity of the process of wave propagation.

The solution of the complete set of equations describing the process of sinusoidal wave propagation [1, 2] give the following general expression for the dependence of the real part of sound velocity u on the frequency f [3]:

$$u^2(f) = u^2(0)[1 + a\Theta + O(\Theta^2)].$$

The value of $\Theta = \omega\tau = 2\pi f\tau$ is defined by the relaxation time τ and sound frequency f; a is an empirical parameter which may be calculated using the selected model. Although the foregoing relation points to the existence of the frequency dependence of the sound velocity, under normal conditions this dependence may be observed only at very high frequencies in excess of 1 GHz. It may show up at lower frequencies as well, in a medium with high fluctuations of density. Such conditions arise in the vicinity of the critical point. As a rule, measurements of the velocity of sound in organic liquids performed at frequencies of the order of 1–5 MHz fail to reveal dispersion; therefore, the velocity of sound in this frequency range may be treated as a thermodynamic quantity facilitating the acquisition of reliable information about the elastic and caloric properties of liquid.

This possibility is based on the fundamental ratio of equilibrium thermodynamics [4] which relates the elastic and caloric properties,

$$\frac{c_p}{c_V} = \frac{\beta_T}{\beta_S} = \gamma. \tag{1}$$

Here, c_p and c_V denote the isobaric and isochoric specific heat capacity, respectively; and β_T and β_S denote the isothermal and adiabatic compressibility of matter, respectively, defined by the known formulas

$$\beta_T = \frac{1}{\rho}\left(\frac{\partial\rho}{\partial p}\right)_T, \quad \beta_S = \frac{1}{\rho}\left(\frac{\partial\rho}{\partial p}\right)_S.$$

The adiabatic behavior of the process of propagation of ultrasonic waves in a relatively wide frequency range makes it possible to use the data on the sound velocity for determining the adiabatic compressibility of liquid

$$\beta_S = \frac{1}{\rho u^2} \tag{2}$$

and the heat capacity ratio

$$\gamma = 1 + \frac{u^2\alpha_P^2 T}{c_p}. \tag{3}$$

In the foregoing formulas, ρ is the density of liquid, and α_P is the isobaric coefficient of thermal expansion.

It is of special interest to study the correlation of the thermodynamic properties of liquid on the saturation curve, where they are a function of only one independent variable, i.e., temperature. The increased stability of each phase of the system on the saturation curve with respect to low-amplitude isentropic perturbations [5] leads one to assume that the process of ultrasonic propagation in a medium does not disturb the phase equilibrium, at least, away from the critical point.

One can complement formulas (1)–(3) with the relation relating the isobaric coefficient of thermal expansion of liquid α_P to the coefficient of thermal expansion along the equilibrium curve α_s and the thermal coefficient of saturated vapor pressure dp_s/dT,

$$\alpha_P = \alpha_s + \beta_T\frac{dp_s}{dT}, \tag{4}$$

where

$$\alpha_P = -\frac{1}{\rho}\left(\frac{\partial\rho}{\partial T}\right)_P, \quad \alpha_s = -\frac{1}{\rho}\left(\frac{\partial\rho}{\partial T}\right)_s,$$

and derive the set of thermodynamic equations (1)–(4) for the calculation of the entire spectrum of the caloric and elastic properties of matter on the saturation curve in the liquid or vapor phase by the experimental data on the density, isobaric heat capacity, saturated vapor pressure, and sound velocity.

Under these conditions, reliable experimental data on the sound velocity at frequencies away from the dispersion region for a wide range of parameters of state are of obvious interest. They are of essential importance from the standpoint of successful solution of various problems associated with the physics of condensed state of matter [1, 2, 4, 6].

Systematic investigations of the velocity of sound in liquids on the saturation curve have been under way for quite some time. They were initiated by the Laboratory of Molecular Acoustics of the Moscow Regional Pedagogical Institute (MOPI). Acoustic investigations of organic liquids by the optical method were performed in this laboratory for many years. The velocity of sound was measured in the megahertz frequency range in both the liquid and vapor phases up to the critical point. The results of these investigations were generalized and given in the well-known monograph by V.F. Nozdrev on *The Uses of Ultrasonics in Molecular Physics* [7]. Given in this monograph are the results of measurements of the sound velocity in a liquid on the saturation curve in organic substances belonging to different homologous series such as isopentane (20–160°C), *n*-hexane (–70–240°C), *n*-heptane (–70–260°C), toluene (–70–180°C), benzene (0–50°C), bromobenzene (–30–40°C), nitrobenzene (6–50°C), chlorobenzene (–44–40°C), methyl alcohol (20–240°C), ethyl alcohol (20–240°C), propyl alcohol (20–240°C), isopropyl alcohol (40–240°C), butyl alcohol (–50–280°C), isobutyl alcohol (20–280°C), and isoamyl alcohol (20–280°C). Also given in the monograph are data of measurements of the velocity of sound in saturated vapors of *n*-hexane (120–240°C), *n*-heptane (153–247°C), toluene (219–288°C), propyl alcohol (125–250°C), butyl alcohol (170–290°C), isopropyl alcohol (152–250°C), isobutyl alcohol (163–283.4°C), and isoamyl alcohol (185–292°C). The error of the measurement results was estimated at 1–3% [7]. In fact, the real measurement error was much higher. In a number of cases, it exceeded several tens of percent. For many years, the data obtained at the MOPI laboratory were the only source of information about the temperature-related features in the behavior of the sound velocity on the liquid–vapor equilibrium curve. However, they were hardly employed in thermodynamic calculations because of their inadequate accuracy. The low accuracy of the sound velocity data given in [7] is apparently due to serious technical difficulties arising in measuring the sound velocity by the optical method at high temperatures and pressures, as well as to the inadequate purity of the objects of investigation.

More recent uses of precision methods of measurement of the sound velocity [8, 9] led one to conclude that the velocity of sound in a dispersionless region is an important thermodynamic parameter [3, 10–15]. This resulted in the emergence of a large number of studies in which the experimental data on the sound velocity were used to search for the equation of state for matter [16, 17] and to refine the values of fundamental thermodynamic constants [18].

Note that the majority of studies devoted to the investigation of the dependence of the sound velocity on the parameters of state are carried out in the single-phase region. The values of the sound velocity at atmospheric pressure, given in the respective papers [6, 14, 15, 19], generally correspond to a narrow range of temperature whose limiting values usually do not exceed the normal boiling point.

Interest in experimental data on the sound velocity in liquid and gaseous media has significantly quickened recently. This is associated with the possibility of using the sound velocity in thermodynamic calculations as a correcting parameter [20–23]. Main attention in the investigations of the sound velocity is given to the study of technically important substances such as liquefied gases, refrigerants, high-molecular paraffins, and organic oils.

The sound velocity in refrigerants was investigated at the Kyoto Institute of Technology under the supervision of T. Takagi [24–28]. The error of measurement results is of the order of 0.1%. Results of investigation of the sound velocity in heavy hydrocarbons may be found in the papers [29–33] of researchers from the laboratory of liquid complexes at the Pau University (France) J.L. Daridon and others. Systematic investigations of the sound velocity are under way at the Imperial College in London under the supervision of Martin Trusler. In his papers, one finds the results of precision measurements of the sound velocity in the gas phase of methane [34], ethane [35], propane [36], *n*-butane [20], and *n*-pentane [21]. These investigations were performed using a spherical acoustic resonator with an error of 0.01%. The error of measurements performed in the liquid phase of *n*-hexane and *n*-hexadecane [37] by the pulse method in the range of 25–100°C is 0.1%.

Unfortunately, little attention is given so far to measurements of the sound velocity on the saturation curve in a wide range of temperatures including the critical point.

Data on the velocity of sound in saturated liquid and vapor for almost the entire equilibrium curve for some technically important organic liquids may be found on the NIST site [38]. However, these data are not the result of direct measurements: they were obtained using high-precision empirical equations of state.

This review is first in a series of papers devoted to the results of ultrasonic investigations performed at the Laboratory of Molecular Acoustics of the KGU. It is the objective of this publication to fill the existing gap in the data on the sound velocity on the saturation curve in organic liquids.

The experimental data on the velocity of ultrasonic waves in organic liquids and their vapors, given in this review, were obtained over a period of the last thirty years using the unified procedure which utilizes the pulse-phase method of fixed distance developed at the KGU. This method enables one to use small amounts of matter and perform measurements in a wide range of parameters of state, including the region adjoining the critical point, with a relatively high accuracy of the measurement results. The data given in tables on the velocity of sound at temperatures above the boiling point are in fact primary data. They were obtained by interpolation within a narrow temperature range by three experimentally obtained values using Lagrange's formula

$$u = u_1\frac{(t-t_2)(t-t_3)}{(t_1-t_2)(t_1-t_3)} + u_2\frac{(t-t_1)(t-t_3)}{(t_2-t_1)(t_2-t_3)} + u_3\frac{(t-t_1)(t-t_2)}{(t_3-t_1)(t_3-t_2)},$$

where u_1, u_2, and u_3 are experimentally obtained values of sound velocity at temperatures t_1, t_2, and t_3, respectively. The sound velocity u was determined for integral values of t close to temperature t_2 on condition that $|t_3 - t_1| \leq 10°C$.

2. DESCRIPTION OF THE EXPERIMENTAL FACILITY

The pulse method of investigation of the acoustic properties of matter has received a fairly wide acceptance. The method consists essentially in the determination of the time of delay of ultrasonic signals in the medium being investigated and in measuring the amplitude ratio of the initial and transmitted signals.

The pulse-phase ultrasonic facility [39, 40] developed at the KGU is designed for studying the acoustic characteristics of liquids and their vapors in a wide range of parameters of state, namely, from –80 to +400°C and from 0.1 MPa to 60 MPa. In more recent studies, the upper pressure limit was raised to 600 MPa. The employed method of measurements of the sound velocity is a variety of the direct pulse method. Its further improvement is associated with the use of modern equipment [41, 42].

We will dwell on the description of the basic principles and characteristic features of the employed method and assess the accuracy of measurements of the sound velocity.

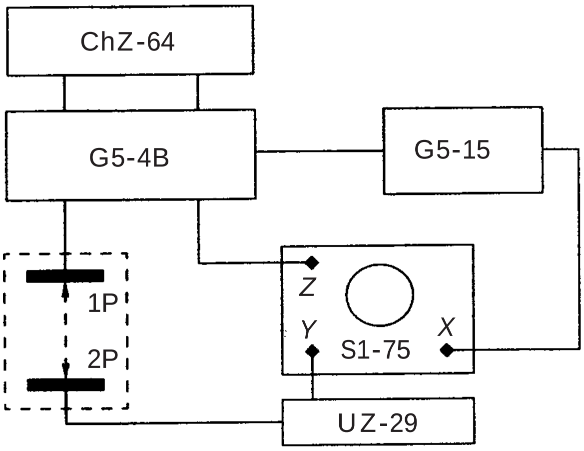

Fig. 1. A block diagram of the experimental facility: for designations, see the text.

2.1. Acoustic Cell and the Electronic Part of the Measuring Setup

An acoustic cell placed in the liquid to be investigated consists of two identical piezoelectric ceramic (or piezoelectric quartz crystal) plates arranged in parallel at a calibrated distance L. The distance between the piezoelectric-crystal plates was measured by an IZV-2 comparator within 2 or 3 µm. At other temperatures according to available literature data and the data of own measurements of the coefficient of thermal expansion of the cell material β, a correction for thermal expansion of the cell was introduced.

A square pulse from one of the channels of a G5-4B two-channel generator (G5-60, G5-65) is applied to one of the piezoelectric-crystal plates (1P, Fig. 1) which is transmitting. The duration of the excitation square pulse is taken to be equal to half the natural period of the piezoelectric-crystal plate. The other, receiving, plate (2P, Fig. 1) is excited by an ultrasonic signal transmitted through the medium being investigated. The arising electric signal is amplified by a UZ-29 wide-band amplifier and delivered to the *Y*-input of an S1-75 oscillograph.

The pulse from the second channel of the G5-4B generator may be delayed relative to the pulse of the first channel. The delay time is varied in a wide range and measured by a ChZ-64 frequency meter (Fig. 1). This pulse is applied to the cathode of the oscillograph CRT (to the *Z*-input) and serves as a moving time mark. The mark width is adjusted by the duration and amplitude of the square pulse of the second channel of the G5-4B generator.

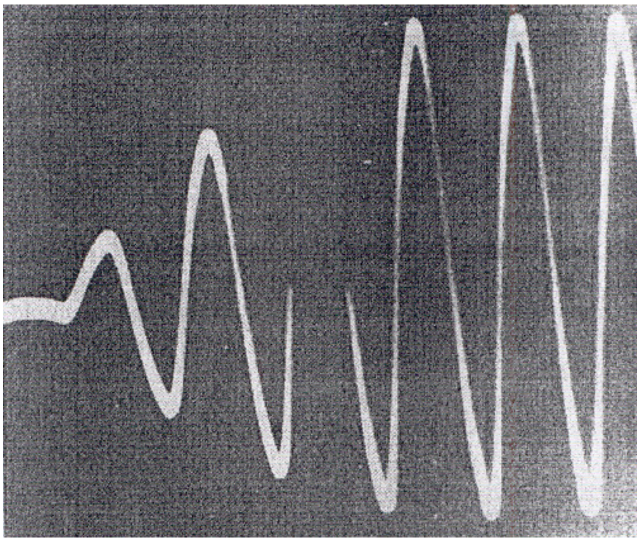

Fig. 2. A photograph of signal observed on the oscillograph display.

In measuring the delay time, the mark (discontinuity of the sweep line) coincides with one of the maxima of the high-frequency component of the signal observed on the oscillograph display (Fig. 2).

The variation by $\Delta\tau$ of the time of transmission of an ultrasonic pulse through the medium being investigated causes the displacement of the time mark along the X-axis by $\Delta x = w\Delta\tau$, where w is the rate of electron beam sweep (Fig. 3). During the same time, the pulse will shift relative to the mark in the Y-direction normal to the sweep line by $\Delta y = (dy/dx)\Delta x$, where (dy/dx) is the quantity characterizing the steepness of the peak of the high-frequency component of the pulse in the region of observation of the mark. Usually, $|dy/dx| \cong$ $\cong 10$; therefore, the observed displacement of the mark relative to the pulse in the Y-direction exceeds significantly its displacement in the X-direction, and this makes it possible to reduce more than twenty-fold the error of indication of the moment of coincidence of the mark with the pulse observed on the display. This is explained by the fact that, when the pulse is displaced relative to the time mark by 0.5 mm in the X-direction, the mark edges move in the Y-direction to a distance of 10 mm away from each other (Figs. 2 and 3). The delay time is read at the instant when the mark edges are at the same height. Under the experimental conditions, a time interval of 0.05 μs corresponded to the mark shift by 0.5 mm. Under this condition, the error, with which the instant of the mark coincidence with the selected maximum of the high-frequency component of the pulse is determined, is 2 to 3 ns, as in the case of high-frequency phase methods.

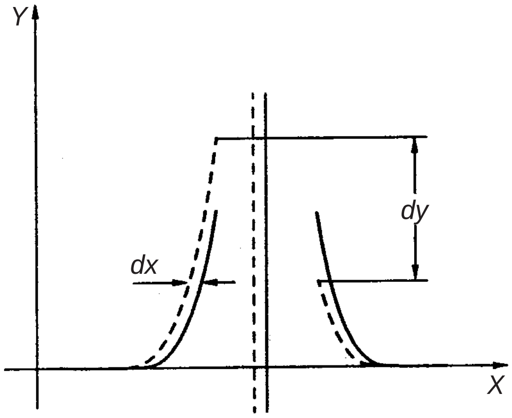

Fig. 3. Comparison of pulse shifts relative to the coordinate axes.

The velocity of propagation of ultrasonic waves in a medium with a fixed distance between the plates is defined by the formula

$$u = \frac{L}{\tau_1 - \tau_0}, \tag{5}$$

in which L is the acoustic path length, τ_1 is the time of complete delay of the pulse of the first channel of the generator relative to that of the second channel, and τ_0 is the delay time dependent on the selected technique of indication of the instant of the mark coincidence with the pulse and of the delay in the electronic part of the setup.

It does not appear possible to theoretically calculate the delay time τ_0. Therefore, its value is usually determined when calibrating the facility against the data on the sound velocity in the reference liquid. When the time mark coincided with the third high-frequency maximum (Fig. 2) of the pulse observed on the oscillograph display, the delay time on the frequency of 1 MHz was $\tau_0 \approx 2.7$ μs.

The delay time τ_0 may vary with the experimental conditions (because of the variation of the thickness of piezoelectric-crystal plate, pulse polarity, length of the connecting cables, selected technique of indication, and so on).

In order to eliminate the delay time τ_0 from the calculation formula, it is necessary to change the delay time of two pulses, namely, the first pulse τ_1 and the second (twice reflected) pulse τ_2. In this case, the sound velocity is calculated by the formula

$$u = \frac{2L}{\tau_2 - \tau_1}. \tag{6}$$

If we take into account the fact that the absolute error of indication (coincidence of the movable time mark with the high-frequency component of the pulse) is $\Delta\tau = \pm 3$ ns and the error of determination of the acoustic base is $\Delta L = \pm 3$ μm, we can arrive at the conclusion that, given the acoustic base length $L = 20$ mm, mean time of complete delay $\tau = 20$ μs, and $\Delta\tau = \pm 0.01$ μs, the total relative error of measurement of the sound velocity amounts to 0.06% (disregarding the reference errors).

2.2. Estimation of Diffraction and Other Effects

The foregoing accuracy of measuring the sound velocity may be attained only in the ideal case in which the displacement of a pulse on the oscillograph display is caused by the variation of the group velocity of ultrasonic signal. However, the transmission of an ultrasonic pulse through the medium being investigated may be accompanied by various effects which lead to deformation of the pulse and cause its additional displacement.

This is associated with the fact that ultrasonic pulses excited by a piezoelectric-crystal plate are not monochromatic. When an ultrasonic pulse propagates in a medium with a frequency-dependent absorption coefficient, its spectral components are attenuated to different degrees, which results in the distortion of the signal shape. A variation of the frequency spectrum causes a phase shift between individual harmonics of the signal and leads to the emergence of phase distortions which affect the precision of the pulse-phase method.

Theoretical calculations of the phase shift were performed by Merkulov and Tret'yakov [43]. They demonstrated that its value was maximal at the leading edge of the pulse and depended significantly on the rise time of the fronts of high-frequency components and on the value of attenuation.

The pulse-phase procedure of measurement of the sound velocity treated by us makes it possible to experimentally estimate the error of measurement of the sound velocity due to phase shift. Indeed, by observing on the oscillograph display the signals caused by repeated reflection of ultrasonic pulse from piezoelectric-crystal plates, one can estimate the effect of the signal path length on the results of measurements of the sound velocity. Obviously, an acoustic pulse that passed a longer distance in a medium must be subjected to greater distortions, and the value of sound velocity calculated from the measurements of the delay time of the first and second pulses must differ from its value obtained by the data of measurements of the delay time of the second and third pulses. In other words, the inequality

$$\Delta\tau_{21} \neq \tau_{32} \tag{7}$$

must be valid.

By checking inequality (7), one can estimate the measurement error due to the variation of the pulse shape. Such a check was made for different classes of organic liquids in a wide range of temperatures and pressures. The investigation results for some liquids are given in Table 1. Analysis of the results reveals that the error of measurement of the sound velocity due to phase distortions does not exceed 0.05%.

Diffraction effects observed in the case of propagation of ultrasonic waves in the medium being investigated may introduce an additional error into the results of measurements of the sound velocity. The procedure of calculation of errors due to diffraction effects is analyzed in [44–47]. This analysis results in the semiempirical expression for the relative error of measurement of the sound velocity defined by diffraction of ultrasonic waves,

$$\frac{\Delta u}{u} = \frac{1}{12}\left(\frac{\lambda}{D}\right)^2 \quad \text{at} \quad L \geq \lambda . \tag{8}$$

In this expression, D is the piezoradiator diameter, λ is the ultrasonic wavelength, and L is the acoustic path length.

Corrections associated with friction (wave–wall) because of significant distance of the acoustic path from the autoclave walls and other surfaces, as well as the presence of adsorption layer on the surface of the piezoelectric-crystal plates, were disregarded. The parallelism of the plates was adjusted by the maximum of the amplitude and by the presence of the "correct" shape of signal (Fig. 2). The introduction of corrections due to the above-identified effects is of significant importance in measuring the absorption coefficient of ultrasonic waves.

Therefore, in the case of standard radiators 20 mm in diameter operating at frequencies of 1–5 MHz and acoustic base length of the cell of 15-20 mm, the overall error of the pulse-phase method without the reference error does not exceed 0.1%.

2.3. Autoclave and Filling System

A high-pressure autoclave is an important part of the experimental facility. The structure of the auto-

Table 1. The ultrasonic velocity measured by three successive pulses

t, °C	P, MPa	τ, µs			u, m/s			$\lvert\varepsilon\rvert$, %
		τ_1	τ_2	τ_3	u_{12}	u_{23}	u_m	
	saturation curve	m-xylene (f = 1.5 MHz, L = 19.745 mm)						
35.4		16.485	47.275	78.055	1282.5	1282.9	1282.7	0.03
60.1		17.765	51.125	84.465	1183.7	1184.4	1184.0	0.06
90.8		19.620	56.675	93.725	1065.7	1065.8	1065.7	0.01
169.3		26.465	77.140	127.86	779.3	778.5	778.9	0.10
		n-chlorotoluene (f = 1.5 MHz, L = 19.745 mm)						
30.1		17.035	43.205	79.340	1266.9	1268.1	1267.5	0.09
60.0		18.475	52.525	86.555	1159.7	1160.4	1160.1	0.06
90.0		20.115	57.445	94.755	1057.8	1058.4	1058.1	0.06
181.8		27.135	78.490	129.84	768.9	769.0	768.9	0.01
		benzene (f = 3.3 MHz, L = 39.390 mm)						
20.4	10	30.110	87.935	145.79	1361.7	1362.4	1362.1	0.05
20.4	50	27.125	78.955	130.80	1520.0	1519.4	1519.7	0.04
20.4	100	24.765	71.865	118.98	1672.6	1672.0	1672.3	0.02
20.5	160	22.465	65.535	108.63	1828.7	1828.0	1828.4	0.02

Note: The following notation is used in Table 1: τ_1, τ_2, and τ_3, delay time of the first, second, and third reflected pulses, respectively; u_{12} and u_{23}, respective ultrasonic velocities; u_m, average velocity for u_{12} and u_{23}; $\lvert\varepsilon\rvert$, relative difference between u_m and u_{12} and u_{23}.

clave employed in measurements of the sound velocity on the saturation curve is given in Fig. 4. The autoclave is a thick-walled cylinder with an inner cylindrical channel, made of 18KhNVA (chrome-nickel-tungsten) stainless steel. The autoclave lid *2* and housing *1* are fastened by bolts through Teflon spacers *8*. The autoclave lid accommodates a device *3* for the evacuation of the measuring chamber and filling it with the liquid under investigation. This latter device consists of a stop needle, a gland, and two unions. Prior to filling, the autoclave was evacuated by a backing pump developing a rarefaction of the order of 10^{-3} mm Hg. The free inner volume of the autoclave was approximately 200 cm^3.

The autoclave design under consideration involved flat electric leads *4* made of copper foil 200 µm thick. Such electric leads enable one to perform acoustic measurements at temperatures up to 450°C and pressures up to 600 bar.

A measuring cell *7* connected to the electric leads by wires *5* was placed in the autoclave. The cell was arranged horizontally to preclude the formation of bubbles in the vicinity of the radiating surface of the plates. The possibility of securing the cell at any height relative to the autoclave bottom enabled one to perform acoustic measurements in both the liquid and vapor phases of matter. The combined use of two cells made it possible to perform simultaneous measurements of the sound velocity in both liquid and saturated vapor. A platinum resistance thermometer *6* was placed alongside the measuring cell.

2.4. System of Thermostatic Control and Temperature Measurement

In the case of high temperatures, the preassigned temperature in the measuring chamber was maintained constant with the aid of an air thermostat. The heater was provided by a cylindrical metal pipe onto which a Nichrome wire was wound on top of a mica substrate. The pipe was closed by two flat lids which were low-power heaters. A stirrer placed into the pipe provided for the necessary temperature field at which no appreciable temperature gradients arose within the autoclave. A system of heaters was placed in a sand bath located in the housing of a TS-24 thermostat. This made for a significant improvement of the heat-insulating characteristics of the system of thermostatic control.

In the first version of the facility, the temperature was preassigned and maintained automatically using a

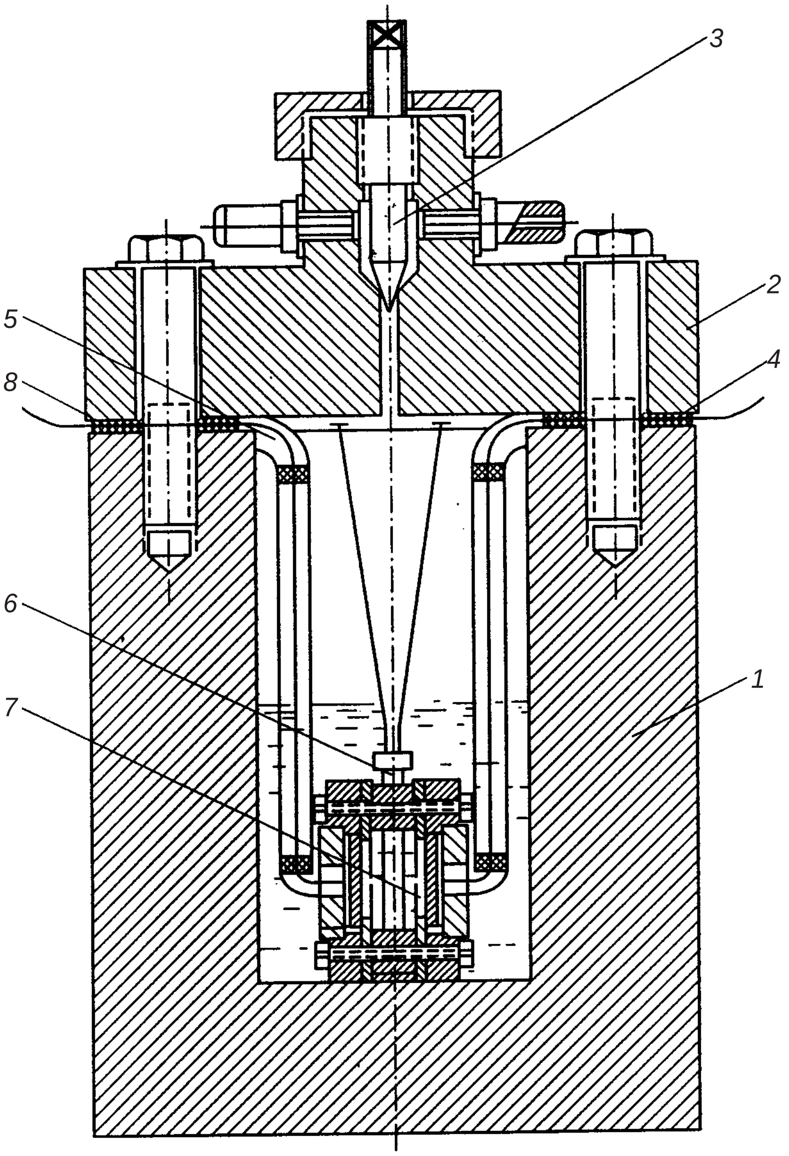

Fig. 4. The structure of autoclave for measuring the sound velocity on the saturation curve: (*1–8*) see the text.

thermostatic switch shown schematically in Fig. 5. A temperature-sensitive element *1* was provided by a platinum resistance thermometer located in the vicinity of a heater *5*. An ac bridge *2* was operated from a common power transformer *6*, which provided for the phase sensitivity of the system. A two-stage amplifier *3* was used to step up the unbalance voltage and deliver it to the grid of a thyratron in whose anode circuit a relay *4* was connected. In the case of coincidence of the phases of the unbalance voltage and of the voltage on the thyratron anode with a positive half-period, the passage of current through the thyratron caused operation of the relay controlling the heater. If the foregoing voltages were opposite in phase, the thyratron was closed and the relay armature released. The high stability of operation was attained owing to the use of a stabilized supply *7*. The thermostatic switch maintained the preassigned temperature constant with an error of ±0.05 °C in the range from 80 to 400°C. At lower temperatures, the TS-24 liquid thermostat was employed. In recent years, a setup involving a VRT-3 thermostatic switch and a KSP-4 multichannel recording potentiometer was used for the purposes of thermostatic control.

The temperature was measured by a platinum resistance thermometer placed in the working volume of the autoclave in the vicinity of the acoustic path. The measuring complex included a P-329 dc bridge and an M1-17 mirror galvanometer. The thermometer was calibrated by way of comparison with a standard

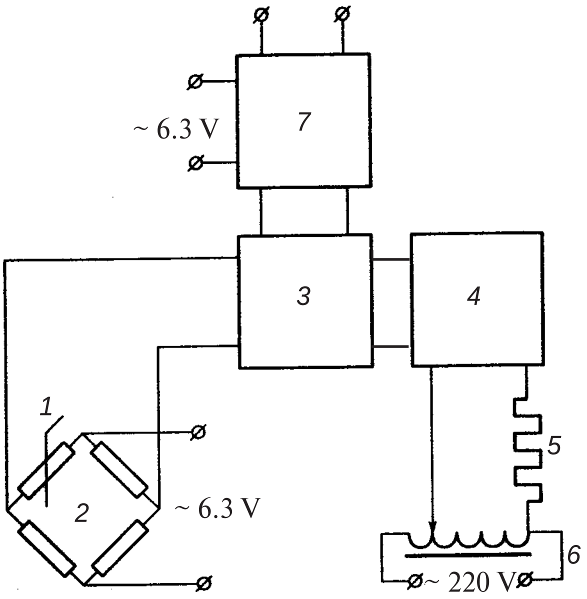

Fig. 5. A block diagram of the system of thermostatic control: (*1–7*) see the text.

thermometer verified at VNIIFTRI (All-Russia Research Inst. of Physicotechnical and Radio Measurements) and by reference points (ice melting point, boiling points of water and other liquids, critical point of reference *n*-heptane, and so on). The calibration provided for reliable measurements of temperature in the range from –50 to +400°C with an error of 0.1°C or less.

2.5. Check Measurements. Estimation of Errors

We will dwell on the assessment of the overall error of measurement of the sound velocity. We can assume the independence of the factor affecting the measurement results and represent the formula for the total error of measurement of the sound velocity as

$$\frac{\Delta u}{u} = \sqrt{\sum_{i=1}^{n} \left(\frac{\Delta u_i}{u}\right)^2}. \qquad (9)$$

The contributions $\Delta u_i/u$ made to the total error of measurement by different factors were as follows: the error of measurement of the delay time, 0.05%; the error of measurement of the acoustic path length, 0.02%; the error of measurement of indication, 0.02%; the error of the employed measurement procedure, 0.05%; and the error of reference with respect to temperature, which amounted to 0.05% at room temperature and increased to 1% in the vicinity of the critical point. The increase in the error of measurement of the sound velocity on approaching the critical point is caused by the significant increase in the temperature coefficient of sound velocity and a significant decrease in the sound velocity proper. Direct calculations of the overall error of measurement of the sound velocity by formula (9) give the following values: 0.1% at temperatures away from the critical point and up to 1% in the vicinity of the critical point.

Table 2. The results of test measurements of the velocity of ultrasonic waves in the liquid phase of toluene (1–3 MHz)

t, °C	u, m/s	
	Our data	Data of Okhotin *et al.* [48]
20	1328	1326.9
30	1284	1283.3
40	1241	1240.2
50	1199	1198.0
60	1157	1156.6
70	1117	1115.7
80	1076	1075.5
90	1036	1035.7
100	996	996.3
110	957	957.0

The calculated values of the error of measurement of the sound velocity are confirmed by the obtained results. For example, it follows from Table 2 that the values of sound velocity in the liquid phase of toluene obtained by us are in good agreement with the data of measurements performed in toluene by another, more precise method of synchro-ring [48]. The results of check measurements of the sound velocity in saturated vapors of benzene and toluene (Table 3) likewise agree with the reliable data given in [49, 50] for a wide temperature range.

2.6. Automation of Measurements

Present-day development of computer equipment and measuring systems made possible a highly efficient automatic ultrasonic facility capable of measuring the acoustic parameters and density of liquid in a wide range of parameters of state. The description of such facility may be found in [51].

General principles of operation of the automatic measuring-and-computer complex reduce to the following. The experimental facility is computer-controlled under the experimenter’s program. After checking the availability of the instrument for service, the computer issues an instruction to take the readings

Table 3. The results of test measurements of the velocity of ultrasonic waves in the saturated vapors of benzene and toluene (1 MHz)

Benzene

t, °C	u, m/s		t, °C	u, m/s	
	Our data	Data of Novikov and Sheludyakov [50]		Our data	Data of Novikov and Sheludyakov [50]
210	181	182.4	260	145	146.0
220	176	177.0	270	134	135.0
230	170	170.5	272	131	132.0
240	163	163.6	280	120	–
250	155	155.3	288	104	–

Toluene

t, °C	u, m/s		t, °C	u, m/s	
	Our data	Data of Will, Froba and Leipertz [49]		Our data	Data of Will, Froba and Leipertz [49]
230	171.4	171.4	280	140.7	141.6
240	167.0	167.4	290	131.2	133.1
250	161.7	162.1	300	119.6	122.3
260	155.8	156.5	310	106.5	108.4
270	148.0	149.5			

of digital instruments, monitor the readings of thermocouples, resistance thermometers, and manganin pressure gage, and calculate the baric and temperature corrections over the acoustic path length. In so doing, the information is displayed about the temperature and pressure in the measuring chamber and the frequency of the probing pulse. After this, the frequency meter is switched over to the mode of measurement of time intervals, and information is delivered to the computer about the time of transmission of the acoustic signal through the medium being investigated. After completion of the measurement cycle, the information is displayed about the temperature and pressure in the medium being investigated, frequency of the probing pulse, ultrasonic velocity, and coefficient of absorption of ultrasonic waves by the medium. The high operation speed of the complex enables one to perform repeated measurements of the acoustic parameters of the object of investigation and statistical processing of the measurement results, with preassigned experimental conditions.

The measuring complex described above was used to investigate the sound velocity in organic liquids, as well as in liquid crystals, polymers, and glasses [41, 42].

3. RESULTS OF MEASUREMENTS OF THE SOUND VELOCITY IN ORGANIC LIQUIDS

Organic liquids as objects of investigation are characterized by the diversity of the molecular structure and by the pattern of intermolecular forces. They are extensively used as heat-transfer agents and refrigerants in power plants, as starting materials in the chemical industry, and in everyday practice. This explains the significant increase in the scientific and practical importance of their all-round investigations.

Liquids of “chemically pure” and “analytically pure” grades were used for investigations. Their purity was controlled by measuring the density, refractive index, and boiling temperature prior to and after the experiment.

Listed in Table 4 in chronological order are the studies [52–92] devoted to measurements of the sound velocity on the saturation curve in the liquid and vapor phases of various organic substances, performed in the Laboratory of Molecular Acoustics of the KGU during the period from 1969 until the present time.

The temperatures, which characterize the saturation curve of investigated substances belonging to three homologous series (saturated hydrocarbons, aromatic compounds, and monatomic aliphatic alcohols), are given in Table 5. The results of measurements of the sound velocity in the liquid and vapor

Table 4. A chronological review of studies devoted to the measurement of sound velocity on the saturation curve, performed at the KGU

Year	Authors	Investigated substances	Temperature range, °C	Year	Authors	Investigated substances	Temperature range, °C
1969	Neruchev, Zotov, Otpushchennikov [52]	*n*-pentane	20–190	1972	Kireev, Otpushchennikov [63]	heptene-1	–118–260
		n-hexane	20–230			nonene-1	30–310
		n-heptane	20–260			decene-1	30–310
		n-octane	20–290			*n*-hexane	–94–60
		n-decane	20–340			*n*-heptane	–80–100
		n-butyl alcohol	20–280			*n*-nonane	–50–160
		isobutyl alcohol	20–270			toluene	–91–100
		n-amyl alcohol	20–310	1972	Korabel’nikov, Ivanova [64]	diethyl ether	0–191
		isoamyl alcohol;	20–300			butyl formate	0–275
		n-hexyl alcohol	20–330	1972	Korabel’nikov, Otpushchennikov, Ivanova [65]	iodobenzene	0–320
1969	Zotov, Neruchev [53]	toluene	20–317			nitrobenzene	10–310
		m-xylene	20–343	1973	Zavarykina, Kireev [66]	pentene-1	–130–180
1969	Pishchikov, Sobolev [54]	diphenyl ether	30–230	1973	Korabel’nikov, Otpushchennikov [67]	isooctane	0–268.5
1969	Zotov [55]	*n*-butyl alcohol–vapor	220–305	1974	Kireev, Melikhov [68]	octane-1	–100–230
		isobutyl alcohol–vapor	210–290	1974	Kireev, Otpushchennikov [69]	diethyl ether	–110–190
		n-amyl alcohol–vapor	240–325			acetone	–90–230
		isoamyl alcohol–vapor	190–320			diisopropyl ether	20–220
1969	Pishchikov [56]	diphenyl	70–80			dibutyl ether	20–300
1969	Tutov [57]	tetralin	20–140			methyl ethyl ketone	20–260
		decalin	20–140			butyl acetate	–70–290
1969	Neruchev [58]	*n*-hexane–vapor	160–233	1974	Korabel’nikov [70]	fluorobenzene	0–284
		n-heptane–vapor	190–266			fluorobenzene–vapor	150–410
		n-octane–vapor	220–293	1975	Timofeev, Otpushchennikov [71]	carbon tetrachloride	20–170
		n-nonane–vapor	260–318	1975	Nikiforov [72]	PMS-150	20–300
1970	Zotov, Otpushchennikov, Neruchev [59]	*n*-xylene	20–340			PMS-400	20–280
						PMS-1000	20–300
		o-xylene	20–350			PES-1	20–300
		butyl benzene	20–350			PES-3	20–240
1970	Zotov, Shoitov [50]	glycerin	20–200			PES-4	20–300
		ethylene glycol	20–190				
		diethylene glycol	20–200				
1970	Pishchikov [61]	dicumyl methane	20–240	1975	Timofeev, Kuz’min [73]	*n*-tetradecane	20–350
1972	Kir’yakov, Otpushchennikov [62]	*n*-dodecane	30–120			*n*-tetradecane–vapor	240–350

Table4. Continue

Year	Authors	Investigated substances	Temperature range, °C	Year	Authors	Investigated substances	Temperature range, °C
1977	Timofeev, [74]	hexyne-1	20–240			*m*-iodotoluene	20–150
		heptine-1	20–270				
		octine-1	20–298				
1977	Timofeev, Otpushchennikov [75]	*n*-octyl alcohol	10–380			*n*-chlorotoluene	20–150
		n-nonyl alcohol	10–390				
1977	Timofeev [76]	*n*-decyl alcohol	20–410				
		n-undecyl alcohol	20–420	1990	Melent’ev, Neruchev [85]	1-chloropropane	–133–157
		n-dodecyl alcohol	20–430			1-chlorohexane	–173–187
1978	Timofeev [77]	hexyne-1–vapor	170–255			1-chloroheptane	–53–117
		heptyne-1–vapor	170–290			3-chloroheptane	–23–157
1978	Korabel’nikov [78]	dioxane	15–308			1-chlorononane	–23–187
		dioxane–vapor	160–308	1993	Shakhov, Mel’nikov, Neruchev, Parfir’ev [86]	*o*-chlorotoluene	–30–160
1982	Timofeev, Nikolaev [79]	cyclopentane	–90–230			2-chloro-*n*-xylene	2–180
		cyclohexane	20–270	1993	Melent’ev [87]	1-chlorohexane	–50–150
		cyclooctane	30–355			1-chloroheptane	–50–150
		cyclopentane–vapor	150–250			1-iodohexane	–50–70
		cyclohexane–vapor	150–250			1-iodoheptane	–40–150
		cyclooctane–vapor	170–380			3-chloroheptane	–40–150
1982	Tsydypov, Otpushchennikov [80]	diphenyl	80–400	1994	Shakhov, Mel’nikov, Davydova [88]	*o*-fluorotoluene	–50–140
1983	Pevnyi [81]	diallyl ether	20–200			*m*-fluorotoluene	–80–120
1983	Timofeev, Alekseev [82]	*n*-propyl alcohol	–120–60			*o*-chlorotoluene	–30–160
		isopropyl alcohol	–85–60			*n*-chlorotoluene	10–160
1984	Tsydypov, Otpushchennikov [83]	benzene	20–260			*m*-iodotoluene	–20–160
		naphthalene	90–340			2,4-dibromotoluene	0–160
		anthracene	220–340			2,4-dichlorotoluene	–10–160
		phenanthrene	110–340	1997	Shakhov, Mel’nikov, Davydova [89]	*o*-fluorochlorobenzene	–40–140
		diphenyl	70–340	1998	Shakhov, Mel’nikov [90]	*m*-fluorobenzo trichloride	–25–220
		cyclohexene	20–260	2002	Shakhov, Neruchev [91]	benzene	10–100
		aniline	20–200			fluorobenzene	
1989	Verveiko, Mel’nikov [84]	chlorobenzene	20–150			chlorobenzene	
		fluorobenzene	20–150			bromobenzene	
		iodobenzene	20–150			iodobenzene	
		2,4-dibromotoluene	20–150			*o*-fluorochlorobenzene	
		2,4-dichlorotoluene	20–150	2003	Bolotnikov, Neruchev [92]	1-chlorohexane 1-iodohexane	20–100

Table 5. The values of temperatures characterizing the saturation curve of investigated liquids by the data of [38]

Substance	T_{melt}, K	T_{boil}, K	T_{cr} , K
n–alkanes and their halogenated compounds			
n–pentane	143.4	309.2	469.7
n–hexane	178.0	341.9	507.6
n–heptane	182.6	371.5	540.2
n–octane	216	398.7	568.7
n–nonane	219.5	423.8	594.6
n–decane	243.3	447.2	617.7
n–undecane	247.4	468.0	639
n–dodecane	263.5	489.2	658
n–tridecane	268	507	675
n–hexadecane	291	554	723
n–nonadecane	304	602.9	755
n–eicosane	310	616.2	786
n–heneicosane	313.4	629.7	778
n–docosane	317	641.8	786
n–tricosane	320	653.2	790
n–tetracosane	324	664.5	800
1–chloropropane	150.2	320	503.2
2–chloropropane	155.97	308	–
1–chlorohexane	179.15	407.7	594.6
1–iodohexane	198.95	454.5	–
3–bromohexane	–	415	–
1–chloroheptane	203.65	432.2	–
3–chloroheptane	–	319	–
1–iodoheptane	225	477.2	–
1–chlorononane	–	476.7	–
aromatic hydrocarbons			
benzene	278.64	353.3	562.05
toluene	178.1	383.8	591.75
m–xylene	225	412.3	617.0
n–xylene	286.4	411.4	616.2
o–xylene	248	417	630.3
ethyl benzene	179	409.3	617.15
butyl benzene	185.1	456	660.5
nitrobenzene	278.9	484	–
fluorobenzene	231.25	358.0	560.1
chlorobenzene	228.0	404.9	632.35
bromobenzene	424.4	429.1	–
o–fluorochlorobenzene	230.5	410.4	–
aliphatic alcohols			
n–butyl alcohol	188	390.6	563.0
n–amyl alcohol	194.95	411	588.1
n–hexyl alcohol	226	430	610.5
n–heptyl alcohol	238.6	448	632.6
n–decyl alcohol	279.6	505	690
n–undecyl alcohol	288.45	–	704
n–dodecyl alcohol	297.0	534.2	719.4
n–tridecyl alcohol	303.5	–	–
n–tetradecyl alcohol	311	562.2	–

phases of the organic compounds of the classes identified above are treated below.

3.1. The Ultrasonic Velocity in Saturated Hydrocarbons and Their Halogenated Compounds

Saturated hydrocarbons (paraffins) represent the simplest series of organic compounds whose molecules consist of atoms of carbon and hydrogen. The first terms in the series, namely, methane, ethane, propane, and butane, under normal conditions are gases. The substitution of hydrogen atom by CH_2 radical results in the formation of a homologous series of liquids of general chemical formula C_nH_{2n+2}.

Starting with butane, paraffin molecules have numerous different isomers. A special place in this series is occupied by liquid *n*-paraffins (*n*-alkanes) which have a linear chain molecular structure. In molecules of *n*-alkanes, carbon atoms form plain staggered chains with spacings

$$R_{C_i - C_{i+1}} = 1.54\ \text{Å}, \quad R_{C_i - C_{i+2}} = 2.50\ \text{Å},$$

$$R_{C_i - C_{i+3}} = 3.90\ \text{Å}$$

and a valence angle C–C–C of the order of 120°. According to the data of [93], this angle is 114° in octane and 120° in a molecule of dodecane. The planes in which hydrogen atoms are located are normal to the molecular axis; in so doing, $R_{\text{C–H}} = 1.092$ Å and the valence angle H–C–H is of the order of 108–115° depending on the homolog number.

In the liquid state in the melting temperature region, the packing of *n*-alkane molecules is similar to rotating cylinders with the average distance between the cylinder axes of 5.6 Å. The average coordination number is approximately six. The temperature rise is accompanied by a decrease in the coordination number and by an increase in the intermolecular spacing. Liquid *n*-alkanes have a uniform short-range order, with the degree of ordering increasing upon transition to higher terms of the series [94, 95].

Studies of vibrational spectra of *n*-alkanes and their isomers [96, 97] revealed that, beginning with *n*-hexane, it does not appear possible to spectroscopically distinguish between *n*-alkanes, i.e., successive addition of a CH_2 group to a molecule of *n*-hexane introduces no marked variations to the form of vibrations of the molecular chain.

Numerous researchers [7, 14, 15, 19, 98–102] measured the velocity of ultrasonic waves in *n*-alkanes on the saturation curve and at atmospheric pressure; however, the majority of measurements relate to a narrow temperature range covering a narrow region of positive or negative temperatures.

Systematic investigations of the velocity of ultrasonic waves in liquid *n*-alkanes were performed at the KGU laboratory by Yu.A. Neruchev, V.V. Zotov [39, 40, 52, 103, 104], V.N. Kuz'min, N.E. Timofeev, Yu. F. Melikhov [41, 73], G.A. Mel'nikov, V.N. Verveiko [42, 105] in almost the entire region of parameters of state. The ultrasonic velocity was measured in the frequency range from 1 to 5 MHz. No dispersion was observed in this frequency range. The maximal error of measurement of the ultrasonic velocity away from the critical point did not exceed 0.1% and increased to 1% in the vicinity of the critical point. An array of experimentally obtained values of the sound velocity in the liquid phase of *n*-alkanes is given in Tables 6–11. For temperatures close to the melting points, the data are approximated by a third-degree polynomial [51]. Given in Tables 6-11 for higher temperatures are in fact primary data on the sound velocity in *n*-alkanes. They were obtained by the interpolation of experimentally obtained values in a narrow temperature range. As was mentioned below, the interpolation was performed by the three-point Lagrange formula in the temperature range whose width did not exceed 10°C. The results of repeated measurements of the sound velocity in *n*-alkanes (Table 12) agree with one another within the error identified above.

Of certain interest was the study of the elastic properties of *n*-alkanes in whose molecules one of the hydrogen atoms is substituted by a halogen atom. The substitution of a hydrogen atom by atoms of Cl, Br, or J results in some variation of the molecular structure; the interatomic spacings in the molecule vary somewhat; the staggered shape of the molecular core remains almost the same. However, in contrast to *n*-alkanes, the molecules of *n*-alkane halides possess a dipole moment. It was demonstrated by Levin [106] that an association of the cyclic or chain type is possible in halogenated *n*-paraffins.

The acoustic properties of halogenated *n*-alkanes have hardly been studied heretofore. This is apparently associated with their high chemical activity and thermal instability [107]. Melent'ev [108] and Bolotnikov [92, 109] performed systematic investigations of the elastic and caloric properties of the liquid phase of *n*-alkane halides and their binary mixtures with *n*-alkanes. The results of measurements of the sound velocity in halogenated *n*-alkanes are given in Table 13.

3.2. The Ultrasonic Velocity in Aromatic Hydrocarbons and Their Halogenated Compounds

The aromatic series of compounds begins with benzene. Benzene molecules have a cyclic structure in the form of a regular plane hexagon at whose vertexes carbon atoms are located. Six hydrogen atoms are held by the carbon atoms by means of covalent bonds in the vicinity of the vertexes of the regular hexagon. According to results of X-ray diffraction studies, the spacing between carbon atoms in liquid benzene is $R_{C-C} = 1.40$ Å, the angle HCC is 120°, and the length of C-H bond is $R_{C-H} = 1.08$ Å [93, 95, 110].

In the solid state, benzene has an orthorhombic lattice. The pattern of relative position of molecules changes little during melting. Just a minor increase in the intermolecular spacing is observed (by approximately 0.26 Å), as well as a decrease in the packing factor from 0.68 to 0.58 and the variation of the mutual orientation of molecules.

In the liquid state, benzene molecules are combined into groups with parallel or mutually perpendicular orientation. Note that X-ray diffraction studies reveal no spacings of 1.54 Å and 1.33 Å which are characteristic of C–C and C=C bonds. This indicates that a special bond of the so-called "aromatic" type [111] is realized in the benzene ring, which differs significantly from aliphatic bonds. Analysis of the results of X-ray diffraction studies of other aromatic compounds (toluene and xylene) may be found in [93, 95, 110, 112].

The molecules of halogenated compounds of benzene, toluene, and xylenes are also based on the benzene ring with parameters of benzene. Atoms of halogens (F, Cl, Br, J), which substitute one of the hydrogen atoms, are located on the continuation of the straight line, which connects C_2 and C_5 atoms, at distances of 2.89 Å to 3.50 Å from the center of the benzene ring depending on the type of halogen.

When a hydrogen atom is substituted by a halogen atom, the molecule center of mass shifts toward the

Table 6. The sound velocity in C_5–C_9 *n*-paraffins (liquid phase)

	u, m/s								
t, °C	*n*-pentane	*t*, °C	*n*-hexane	*t*, °C	*n*-heptane	*t*, °C	*n*-octane	*t*, °C	*n*-nonane
–80	1534.1	–80	1585.7	–80	1623.3				
–60	1430.7	–60	1483.6	–60	1520.4				
–40	1327.4	–40	1382.5	–40	1422.5	–40	1452.2	–40	1487.8
–20	1226.5	–20	1284.7	–20	1329.2	–20	1364.1	–20	1397.8
0	1128.2	0	1190.5	0	1239.8	0	1278.0	0	1310.6
20	1031.7	20	1099.2	20	1153.3	20	1193.3	20	1226.9
40	935.9	40	1010.2	40	1068.9	40	1111.4	40	1148.4
60	839.8	60	921.1	60	984.8	60	1030.5	60	1068.7
80	743.6	80	833.8	80	903.3	80	951.3	80	993.4
100	647.1	100	746.9	100	821.2	100	874.1	100	918.3
110	598.8	110	704.1	110	781.7	110	836.1	110	881.2
120	550.4	120	659.5	120	740.9	120	798.3	120	845.1
130	500.8	130	616.0	130	700.8	130	760.9	130	808.7
140	450.7	140	573.2	140	660.0	140	723.2	140	773.4
150	398.7	150	529.4	150	619.9	150	685.4	150	738.0
160	344.2	160	484.8	160	580.2	160	647.2	160	702.9
170	287.4	170	439.3	170	540.0	170	610.5	170	666.2
175	257.2	180	393.0	180	499.6	180	572.9	180	631.1
180	225.3	190	345.4	190	458.6	190	535.9	190	596.1
181	218.7	200	295.6	200	416.6	200	498.2	200	560.9
182	212.0	210	242.5	210	373.8	210	460.5	210	525.6
183	205.1	215	214.1	220	330.0	220	422.0	220	490.4
184	198.2	220	183.7	230	284.5	230	382.7	230	455.1
185	191.1	221	177.3	240	236.3	240	342.4	240	429.0
186	184.0	222	170.9	245	210.5	250	301.2	250	382.3
187	176.6	223	164.3	250	183.5	260	258.0	260	344.6
188	169.3	224	157.7	251	177.9	270	211.9	270	309.1
189	161.6	225	150.9	252	172.1	275	187.5	280	267.1
190	153.8	226	143.9	253	166.4	280	161.6	290	225.3
191	145.7	227	136.7	254	160.6	281	156.1	295	203.3
192	137.3	228	129.3	255	154.6	282	150.7	300	180.7
193	128.7	229	121.6	256	148.5	283	145.1	305	156.3
194	119.6	230	112.7	257	142.3	284	139.4	310	130.4
195	109.8	231	104.3	258	135.8	285	133.6	311	124.8
196	99.6	232	95.4	259	129.3	286	127.7	312	119.4
		233	86.6	260	122.5	287	121.7	313	113.9
				261	115.7	288	115.5	314	108.4
				262	108.9	289	109.5	315	102.0
				263	101.5	290	102.9	316	95.9
				264	93.1	291	95.5	317	89.8
				265	85.3	292	89.4	318	83.4
				266	76.5	293	82.5	319	77.7
						294	75.0	320	67.8

Table 7. The sound velocity in C_{10}–C_{11} *n*-paraffins (liquid phase)

u, m/s							
t, °C	*n*-decane	*t*, °C	*n*-decane	*t*, °C	*n*-undecane	*t*, °C	*n*-undecane
20	1254.9	300	268.7	20	1280.2	300	329.5
30	1215.2	305	249.6	30	1240.3	305	312.4
40	1176.7	310	229.7	40	1207.8	310	295.0
50	1139.4	315	209.2	50	1164.2	315	277.4
60	1100.2	320	188.0	60	1128.1	320	259.3
70	1064.7	321	183.6	70	1092.1	325	241.0
80	1025.8	322	179.2	80	1055.7	330	222.1
90	990.3	323	174.7	90	1019.9	335	202.6
100	953.3	324	170.3	100	986.5	340	182.4
110	918.1	325	165.7	110	950.8	345	160.9
120	884.0	326	161.5	120	916.9	346	156.5
130	849.3	327	156.5	130	882.8	347	152.0
140	814.9	328	151.8	140	850.6	348	147.5
150	781.3	329	147.1	150	816.2	349	142.9
160	747.2	330	142.4	160	782.1	350	138.1
170	712.9	331	137.7	170	749.8	351	133.6
180	679.2	332	132.8	180	716.3	352	128.6
190	646.1	333	127.4	190	684.2	353	123.3
200	612.8	334	122.5	200	652.0	354	118.3
210	579.7	335	117.3	210	620.6	355	113.6
220	546.3	336	112.5	220	588.0	356	108.3
230	512.7	337	106.9	230	557.0	357	103.0
240	479.6	338	101.3	240	525.0	358	97.5
250	446.0	339	96.0	250	493.2	359	92.0
260	411.8	340	90.2	260	461.1	360	86.0
270	377.4	341	84.3	270	428.8	361	80.4
280	342.3	342	78.3	280	396.1	362	74.1
290	306.2	343	71.9	290	363.3	363	67.6

halogen atom. This shift increases with the mass of the halogen atom. This causes an increase in the effective volume occupied by the molecule of aromatic hydrocarbon and the variation of its other properties.

The acoustic properties of aromatic hydrocarbons and their halogenated compounds were investigated by a number of researchers [113–116]. Investigations of aromatic compounds at the Laboratory of Molecular Acoustics of the KGU were performed by V.V. Zotov, Yu.A. Neruchev, A.V. Korabel'nikov, V.M. Tutov, N.E. Timofeev, G.M. Pan'kevich, Yu.F. Melikhov, V.N. Verveiko, G.A. Mel'nikov, A.V. Shakhov [40–42, 53, 59, 70, 84, 88–91, 117], and others. The results of measurements of the sound velocity on the saturation curve in liquid aromatic hydrocarbons and their halogenated compounds are given in Tables 14–17.

3.3. The Ultrasonic Velocity in Monatomic Alcohols

Aliphatic monatomic alcohols are produced by substituting one of the hydrogen atoms in molecules of *n*-paraffins by OH hydroxyl group. Molecules of *n*-alcohols in the solid state are stretched-out chains [118] which may transform to spirals on approaching the melting point.

Alcohols fall into the category of associated liquids with hydrogen bonds. The degree and pattern of the association of liquid alcohols depend on both the molecular structure and ambient conditions. When the

Table 8. The sound velocity in C_{12} *n*-paraffins (liquid phase)

u, m/s							
t, °C	*n*-dodecane	*t*, °C	*n*-dodecane	*t*, °C	*n*-dodecane	*t*, °C	*n*-dodecane
20	1296.0	170	775.3	325	294.2	369	129.7
30	1258.0	180	744.0	330	277.5	370	124.7
40	1220.8	190	713.1	335	260.4	371	120.1
50	1182.3	200	681.6	340	242.9	372	115.5
60	1145.9	210	651.1	345	225.0	373	110.7
70	1110.8	220	620.9	350	206.4	374	105.8
80	1075.1	230	590.1	355	187.2	375	100.8
90	1038.9	240	559.8	360	167.7	376	95.3
100	1004.2	250	529.4	361	163.6	377	90.4
110	971.0	260	499.2	362	159.5	378	85.4
120	937.2	270	468.5	363	155.4	379	79.9
130	905.5	280	437.8	364	151.3	380	74.1
140	871.1	290	406.5	365	146.9	381	68.0
150	840.2	300	374.8	366	143.0		
160	807.3	310	343.2	367	138.5		

Table 9. The sound velocity in C_{16} *n*-paraffins (liquid phase)

u, m/s							
t, °C	*n*-hexadecane	*t*, °C	*n*-hexadecane	*t*, °C	*n*-hexadecane	*t*, °C	*n*-hexadecane
20	1356.6	130	979.9	240	661.3	350	367.1
30	1318.2	140	950.2	250	633.8	360	339.4
40	1283.9	150	917.6	260	606.7	370	312.6
50	1248.6	160	889.4	270	579.6	380	285.2
60	1209.6	170	858.7	280	552.9	390	256.4
70	1175.2	180	830.9	290	526.3	400	228.2
80	1142.0	190	801.4	300	500.2	410	198.1
90	1106.0	200	774.2	310	474.3	420	166.9
100	1074.2	210	745.6	320	447.5	430	132.6
110	1043.9	220	715.7	330	420.6	440	94.6
120	1009.4	230	688.8	340	393.8		

temperature rises, part of the hydrogen bonds are broken.

According to X-ray data [119], molecules of *n*-alcohols in the liquid state have a linear shape. The linear pattern of molecular chains of *n*-alcohols persists up to $n = 26$ (n is the number of carbon atoms per molecule of alcohol). One arrives at a similar conclusion after studying the molar volume of alcohols as a function of the number of CH_2 groups and after investigating the intensity of anisotropic scattering of light.

The intermolecular interaction in *n*-alcohols is defined by Van der Waals' forces and forces responsible for hydrogen bonds. To a first approximation, one can conclude that the hydrogen bond contribution to the total energy of intermolecular forces of different alcohols at a preassigned temperature is the same. The energy of intermolecular interaction increases with the number of the term in the series. One arrives at this conclusion as a result of analysis of the variation of the heat of evaporation upon an increase in the number of CH_2 groups per molecule of alcohol. It is further confirmed by the behavior of the critical temperature, molar volume, activation energy of viscous flow, and molar refraction in the series of *n*-alcohols.

It follows from the foregoing that normal monatomic aliphatic alcohols have similar structures and

Table 10. The sound velocity in C_{13} and C_{19}–C_{21} *n*-paraffins (liquid phase)

u, m/s							
t, °C	*n*-tridecane	*t*, °C	*n*-nanodecane	*t*, °C	*n*-eicosane	*t*, °C	*n*-heneicosane
30	1281.3	40	1315.1	50	1288.8	60	1261.7
40	1242.0	50	1279.8	60	1254.5	70	1228.0
50	1204.5	60	1244.8	70	1219.3	80	1194.0
60	1168.5	70	1209.6	80	1187.5	90	1161.0
70	1132.0	80	1176.8	90	1154.2	100	1128.0
80	1096.4	90	1144.3	100	1122.1	110	1097.0
90	1063.4	100	1112.0	110	1090.1	120	1066.7
100	1029.1	110	1081.3	120	1059.8	130	1036.8
110	995.6	120	1049.3	130	1029.5	140	1007.8
120	962.5	130	1017.4	140	998.8	150	977.7
130	929.7	140	987.5	150	970.4	160	949.0
140	897.2	150	957.9	160	941.6	170	922.5
150	865.0	160	929.0	170	913.1	180	895.4
160	834.2	170	900.2	180	884.9	190	868.5
170	801.7	180	871.7	190	857.5	200	842.0
180	771.3	190	843.9	200	830.3		
		200	816.7				

Table 11. The sound velocity in C_{22}–C_{23} *n*-paraffins (liquid phase)

u, m/s					
t, °C	*n*-docosane	*t*, °C	*n*-tricosane	*t*, °C	*n*-tetracosane
60	1265.5	60	1274.8	60	1280.5
70	1233.8	70	1241.9	70	1247.5
80	1200.5	80	1208.4	80	1215.0
90	1168.7	90	1176.0	90	1183.2
100	1136.5	100	1145.5	100	1152.8
110	1106.0	110	1114.2	110	1121.9
120	1075.6	120	1083.9	120	1091.0
130	1045.0	130	1053.8	130	1061.5
140	1015.6	140	1024.7	140	1032.2
150	986.2	150	996.4	150	1003.4
160	957.6	160	967.8	160	975.2
170	930.6	170	940.6	170	948.8
180	903.3	180	913.2	180	921.7
190	876.8	190	887.3	190	895.2
200	850.4	200	860.3	200	868.5

bonds and differ from one another only by the intensity of intermolecular forces.

All regularities revealed for *n*-alcohols are valid for isoalcohols as well. Therefore, aliphatic isoalcohols may also be combined into one group of compounds by the pattern of intermolecular interaction and molecular structure.

The acoustic methods were employed to investigate the homologous series of saturated monatomic alcohols in considerable detail. A review of these investigations may be found in [120].

Systematic measurements of the sound velocity in the liquid and vapor phases of monatomic alcohols on the saturation curve including the critical region were

Table 12. The results of repeated measurements of the sound velocity in *n*-hexane and *n*-nonane

t, °C	*u*, m/s					
	n-hexane			*n*-nonane		
	[108]	[104]	Our data	[109]	[104]	Our data
20	1098.1	1098	1099.2	1228.0	1227	1226.9
30	1054.3	1054	1054.4	1190.8	1187	1187.5
40	1009.9	1010	1010.2	1149.3	1148	1148.4
50	965.7	966	965.7	1109.2	1109	1109.0
60	921.3	921	921.1	1069.0	1069	1068.7
70	977.8	878	877.9	1030.4	1030	1030.3
80	834.0	834	833.8	992.1	993	993.4
90	790.3	790	789.8	955.0	955	954.6
100	746.6	747	746.9	918.2	918	918.3
110				881.6	881	881.2
120				845.1	845	845.1
130				809.6	809	808.7
140				774.2	773	773.4
150				738.3	738	738.0

performed by V.V. Zotov, Yu.A. Neruchev, and N.E. Timofeev [40, 52, 55, 75, 76]. The measurement results are given in Tables 18 and 19.

3.4. Analysis of Experimental Results

In order to gain a general impression of the pattern of temperature dependence of the sound velocity in the investigated liquids, we can turn to Fig. 6 which gives the temperature dependences $u = f(T_{\text{cr}} - T)$ of the sound velocity in *n*-hexane, benzene, and *n*-hexyl alcohol. The molecules of these alcohols contain the same number of carbon atoms ($n = 6$) while representing three homologous series. It follows from Fig. 6 that the pattern of the temperature dependence of the sound velocity in these liquids is almost the same, and the values proper are close to one another. In a relatively wide temperature range, the sound velocity in the liquid phase of *n*-hexane and benzene increases almost linearly with increasing temperature. A significant deviation from linearity is observed only in the region immediately adjacent to the critical point, where the temperature coefficient of sound velocity increases by a factor of two or three compared to the values in the linear region. The temperature dependence of the sound velocity in *n*-hexyl alcohol differs from the $u(T)$ dependences in *n*-hexane and benzene. It exhibits a nonlinear pattern in almost the entire temperature range. The observed nonlinearity is apparently associated with the process of breakage of hydrogen bonds present in alcohols, the intensity of which increases with temperature. On approaching the critical point, the pattern of the temperature dependence of the sound velocity in the liquids being treated is almost the same.

Analysis of the data on the thermal properties of investigated liquids representing three homologous series of organic substances leads one to reveal some special features associated with the difference in the molecular structures and pattern of intermolecular forces.

It is doubtless of interest to study the effect produced on the thermal properties of organic liquids by the introduction of halogen atoms and OH hydroxyl group into their molecules. Such investigations were performed by a number of researchers [108, 109, 117]. Their results were discussed in detail in various publications. We will. summarize briefly the obtained results.

Comparison of the thermal properties of *n*-alkanes and alkyl benzenes and their halogenated compounds reveals that the substitution of a hydrogen atom by a halogen atom results in a decrease in the temperature

Table 13. The sound velocity in halogenated *n*-paraffins (liquid phase)

t, °C	*u*, m/s								
	1-chloro-propane	2-chloro-propane	1-chloro-hexane	1-iodo-hexane	3-bromo-hexane	1-chloro-hexane	3-chloro-heptane	1-iodo-heptane	1-chloro-nonane
20	1085.8	1013.6	1216.2	1045.5	1094.7	1247.8	1233.3	1077.4	1295.5
40	998.4	920.1	1140.6	989.1	1034.2	1172.8	1151.6	1021.6	1220.8
60	913.9	839.2	1069.4	934.6	969.6	1101.7	1076.4	965.4	1150.5
80	830.7	759.5	996.4	879.3	907.6	1030.7	1007.9	912.8	1081.5
100	746.9	686.0	923.4	825.5	844.6	961.9		863.1	1014.0
120	665.9		857.9	776.7	780.2	896.7		808.9	949.2
140			789.6	725.6	730.2	828.3		757.8	884.5

Table 14. The sound velocity in the liquid phase of aromatic hydrocarbons (xylenes and nitrobenzene)

u, m/s							
t, °C	m-xylene	t, °C	n-xylene	t, °C	o-xylene	t, °C	nitrobenzene
–40	1597.9						
–20	1511.5			–20	1520		
0	1426.9			0	1442		
20	1344.0	20	1332	20	1363	20	1475
40	1262.8	40	1249	40	1285	40	1405
60	1184.6	60	1169	60	1208	60	1335
80	1104.0	80	1091	80	1130	80	1267
100	1027.7	100	1016	100	1056	100	1200
120	953.9	120	941	120	983	120	1134
140	882.9	140	869	140	912	140	1069
160	811.5	160	798	160	841	160	1005
180	738.7	180	728	180	771	180	942
200	668.0	200	657	200	699	200	879
220	596.9	220	587	220	630	220	819
240	526.4	240	518	240	561	240	760
260	454.1	260	446	260	490	260	701
280	379.2	280	372	280	419	280	641
300	300.7	300	293	300	343	300	579
305	279.6	305	272	305	324	310	547
310	258.2	310	251	310	304		
320	212.8	320	205	320	263		
321	208.1	321	201	325	241		
322	203.3	322	196	330	218		
323	198.5	323	191	335	195		
324	193.7	324	186	340	170		
325	187.7	325	181	341	165		
326	183.7	326	176	342	160		
327	178.7	327	171	343	154		
328	173.5	328	166	344	148		
329	168.2	329	161	345	143		
330	163.0	330	156	346	137		
331	157.7	331	150	347	132		
332	152.3	332	145	348	126		
333	146.8	333	139	349	120		
334	141.2	334	133	350	114		
335	135.3	335	127	351	108		
336	129.6	336	122	352	101		
337	123.2	337	116	353	95		
338	117.2	338	109	354	88		
339	111.0	339	103	355	81		
340	104.6	340	96				
341	97.8	341	89				
342	90.8	342	82				
343	83.1						

Table 15. The sound velocity in the liquid phase of aromatic hydrocarbons (benzene, toluene, ethyl benzene, and butyl benzene)

u, m/s							
t, °C	benzene	*t*, °C	toluene	*t*, °C	ethyl benzene	*t*, °C	butyl benzene
20	1323	20	1328	20	1339	20	1355
30	1275	30	1284	30	1298	30	1313
40	1230	40	1241	40	1256	40	1275
50	1184	50	1199	50	1215	50	1237
60	1139	60	1157	60	1177	60	1201
70	1095	70	1117	70	1138	70	1164
80	1051	80	1076	80	1100	80	1127
90	1009	90	1036	90	1061	90	1091
100	966	100	996	100	1023	100	1056
110	924	110	957	110	986	110	1022
120	882	120	919	120	950	120	987
130	841	130	880	130	914	130	954
140	800	140	842	140	878	140	920
150	759	150	804	150	842	150	887
160	717	160	767	160	805	160	855
170	675	170	728	170	768	170	822
180	634	180	691	180	733	180	789
190	593	190	652	190	698	190	758
200	550	200	615	200	664	200	725
210	508	210	577	210	629	210	692
220	465	220	539	220	593	220	661
230	421	230	500	230	554	230	630
240	377	240	462	240	520	240	599
250	329	250	423	250	484	250	568
260	279	260	382	260	448	260	536
270	225	270	340	270	411	270	502
271	219	280	296	280	373	280	471
272	213	290	250	290	335	290	439
273	207	295	225	300	294	300	407
274	201	300	200	310	253	310	374
275	195	305	173	320	210	320	341
276	189	310	143	330	161	330	307
277	183	311	137	335	132	340	271
278	176	312	131			350	235
279	170	313	124			360	197
280	163	314	118				
281	156	315	109				
282	149	316	102				
283	142	317	93				
284	135						
285	127						
286	119						
287	109						
288	99						

Table 16. The sound velocity in halogenated compounds of benzene (liquid phase)

t, °C	u, m/s						
	fluorobenzene	chlorobenzene	bromobenzene	iodobenzene	*o*–fluorochlorobenzene	*m*–fluorobenzotrichloride	*n*–fluorobenzotrichloride
–40	1445.6	1525.5			1434.6		
–30	1400.3	1483.6	1335.6	1245.2	1396.4		
–20	1355.7	1442.7	1301.3	1218.8	1358.6	1358.5	
–10	1311.9	1402.6	1267.5	1192.3	1321.1	1325.0	1329.4
0	1268.9	1363.3	1234.3	1166.0	1284.0	1291.5	1294.1
10	1226.5	1324.8	1201.6	1139.7	1247.1	1258.2	1260.1
20	1184.7	1286.8	1169.3	1113.6	1211.2	1225.2	1226.3
30	1143.5	1249.5	1137.6	1087.5	1175.3	1192.4	1192.5
40	1102.9	1212.6	1106.4	1061.5	1139.8	1160.4	1159.4
50	1062.8	1176.2	1075.6	1035.6	1105.2	1128.1	1127.0
60	1023.1	1140.1	1045.3	1009.8	1071.1	1097.6	1095.2
70	983.8	1104.2	1015.4	984.2	1038.0	1067.1	1064.1
80	944.8	1068.6	985.9	958.6	1005.5	1037.2	1033.6
90	906.2	1033.0	956.8	933.2	972.8	1008.0	1003.6
100	867.8	997.6	928.2	908.0	940.1	979.3	974.3
110	829.7	962.0	899.8	882.9	910.2	951.2	945.6
120	791.7	926.4	871.8	858.0	880.0	923.7	917.5
130	753.9	890.6	844.2	833.3	850.2	896.8	889.9
140			816.9	808.8		870.4	862.9
150			789.9	784.6		844.5	836.5
160			763.2	760.6		819.2	810.7
170				736.8		794.3	785.4
180				713.4		770.1	760.7
190				690.3		746.3	736.5
200						723.0	712.9
210						700.3	689.8
220						678.0	667.2

coefficient of sound velocity, whose variation is the greater, the greater the mass of halogen. In so doing, the pattern of the dependence on temperature remains by and large the same. As the temperature rises, the sound velocity decreases by a close-to-linear law (Figs. 7 and 8). In aliphatic alcohols (Fig. 9), the temperature coefficient of sound velocity hardly varies with increasing molecular mass of liquid.

A study of the molar velocity of sound which is defined by the formula $U_m = uM^{1/2}$ enables one to reveal the effect made by halogen introduced into molecules of liquid on the intensity of intermolecular forces. Comparison of the dependences $U_m = f(T)$ for investigated liquids (Figs. 10 and 11) reveals that the introduction of a halogen atom into a molecule of hydrocarbon causes an increase in the molar velocity of sound and, consequently, leads to an increase in the intensity of intermolecular forces.

The exception is provided by the dependences $U_m = f(T)$ for benzene and fluorobenzene (Fig. 11), which coincide with each other almost completely in the entire investigated temperature range. Note that these liquids are characterized by close boiling temperatures, coefficients of expansion, and other quantities closely related to the energy of intermolecular forces. The equality of the values of the molar velocity of sound in these liquids is apparently due to the fact that the high electronegativity of a fluorine atom leading to an increase in the intensity of intermolecular forces is compensated for by the large distance between molecules.

Table 17. The sound velocity in halogenated compounds of toluene (liquid phase)

	u, m/s						
t, °C	*o*–chloro-toluene	*n*–chloro-toluene	*m*–iodo-toluene	2,4–dichloro-toluene	2,4–dibromo-toluene	*o*–fluoro-toluene	*m*–fluoro-toluene
–80							1662.9
–70							1617.0
–60						1588.1	1571.6
–50						1535.3	1526.7
–40						1486.4	1482.2
–30	1507.7					1441.3	1438.2
–20	1469.6		1262.2			1400.1	1394.8
–10	1431.8		1232.1	1408.4		1357.8	1351.8
0	1394.2		1202.4	1373.3	1227.7	1316.1	1309.3
10	1357.0	1341.5	1173.2	1339.7	1195.8	1274.8	1267.3
20	1320.0	1305.1	1144.5	1307.5	1166.6	1233.9	1225.8
30	1283.3	1269.1	1116.2	1273.6	1139.9	1193.5	1184.8
40	1246.9	1233.4	1088.4	1241.5	1113.4	1153.4	1144.4
50	1210.7	1198.1	1061.1	1209.8	1087.4	1113.8	1104.5
60	1174.8	1163.1	1034.1	1178.4	1061.9	1074.6	1065.2
70	1139.2	1128.4	1007.6	1147.3	1036.7	1035.8	1026.5
80	1103.9	1094.1	981.6	1116.7	1012.0	997.4	988.3
90	1068.9	1060.1	956.0	1086.4	987.7	959.5	950.7
100	1034.1	1026.5	930.0	1056.4	963.9	921.9	913.7
110	999.6	993.2	906.0	1026.8	940.5	884.8	877.4
120	965.4	960.3	881.7	997.5	917.5	848.1	841.6
130	931.4	927.7	857.7	968.7	894.9	811.8	
140	897.7	895.5	834.2	940.1	872.8	775.6	
150	864.3	863.6	811.1	911.9	851.1		
160	831.1	832.0	788.4	884.1	829.8		

The increase in the molar velocity of sound with increasing intensity of intermolecular forces shows up clearly in aliphatic alcohols as well. It follows from the data given in Fig. 12 that an increase in the size of an alcohol molecule leads to an increase in the molar velocity of sound.

3.5. The Ultrasonic Velocity in the Vicinity of the Critical Point

Investigations of the temperature dependence of the sound velocity in the vicinity of the critical point were begun quite some time ago [11]. As a result, it was found that, when the critical point is approached, the temperature coefficient of sound velocity increases abruptly, and the sound velocity and adiabatic compressibility assume extreme values. The thermodynamic theory of Gibbs and Landau, which is successfully developed by Novikov [121, 122], leads one to conclude that the sound velocity at the critical point assumes zero value. However, the special features of the behavior of the velocity of sound in the liquid and vapor phases in the region adjoining the critical point have not yet been adequately studied for the majority of organic substances.

The experimental difficulties arising when the acoustic methods are employed to investigate matter in the above-identified region of states are caused by the fact that, because of the anomalously high compressibility, the results of measurements in the vicinity of the critical point are significantly affected by various factors, in particular, by the gravitational effect [123–125]. Most probably, the critical state is realized only in a thin layer in the vicinity of the interface. In addition, the process of propagation of sound in the vicinity of the critical point may bring about absolutely unstable states of matter beyond the spin-

Table 18. The sound velocity in aliphatic alcohols (liquid phase)

u, m/s									
t, °C	*n*-amyl alcohol	*t*, °C	isoamyl alcohol	*t*, °C	*n*-butyl alcohol	*t*, °C	*n*-butyl alcohol	*t*, °C	*sec*-hexyl alcohol
30	1258.0	30	1220.0	30	1223.9	30	1285.0	30	1240.8
50	1191.6	50	1152.9	50	1156.4	50	1219.2	50	1167.3
70	1124.4	70	1086.4	70	1090.8	70	1152.1	70	1095.5
90	1057.1	90	1019.3	90	1022.9	90	1085.1	90	1023.6
100	1023.2	100	984.9	100	988.4	100	1053.3	100	986.7
110	988.9	110	951.2	110	954.0	110	1020.1	110	950.0
120	955.1	120	916.6	120	918.4	120	986.0	120	913.3
130	920.4	130	881.3	130	881.3	130	951.7	130	875.8
140	884.2	140	845.9	140	843.6	140	917.8	140	838.6
150	847.4	150	808.4	150	804.9	150	881.7	150	800.3
160	810.2	160	771.1	160	765.1	160	846.1	160	761.4
170	772.4	170	732.9	170	724.9	170	810.5	170	723.0
180	732.8	180	693.9	180	683.6	180	773.5	180	683.8
190	693.3	190	654.3	190	640.2	190	736.1	190	643.4
200	653.1	200	614.2	200	597.3	200	697.8	200	603.3
210	612.4	210	573.1	210	552.4	210	659.8	210	562.4
220	570.5	220	531.0	220	506.6	220	621.4	220	519.7
230	529.7	230	487.6	230	458.5	230	583.4	230	474.8
240	486.3	240	443.8	240	409.0	240	543.5	240	426.4
250	442.8	250	398.4	250	356.8	250	503.8	250	366.6
260	397.6	260	352.0	260	301.9	260	463.3	260	304.0
270	350.5	270	302.5	265	272.9	270	422.2	265	272.9
280	299.7	280	250.3	270	242.5	280	379.9	270	240.1
290	247.1	290	193.4	271	236.1	290	336.6	275	203.9
295	219.4	291	187.3	272	229.8	300	291.4	280	164.1
300	189.7	292	181.1	273	222.9	310	243.8	285	131.2
301	183.5	293	174.9	274	216.6	315	218.7		
302	177.2	294	168.5	275	210.0	320	192.2		
303	170.7	295	162.0	276	203.5	321	187.2		
304	164.4	296	155.4	277	196.7	322	181.6		
305	157.7	297	148.5	278	189.6	323	176.2		
306	150.8	298	141.5	279	182.4	324	170.3		
307	144.0	299	134.3	280	175.3	325	164.9		
308	136.5	300	126.8	281	167.7	326	159.1		
309	129.6	301	119.3	282	160.1	327	153.4		
310	121.5	302	110.5	283	152.2	328	147.5		
311	114.2	303	102.5	284	144.3	329	141.4		
312	106.8	304	95.1	285	135.9	330	135.1		
313	98.2			286	127.6	331	129.1		
				287	118.4	332	122.8		
				288	107.9	333	116.9		
						334	109.2		
						335	103.2		
						336	96.8		

Table 19. The sound velocity in aliphatic alcohols (liquid phase)

						u, m/s							
t, °C	*tert*-hexyl alcohol	*t*, °C	*n*-heptyl alcohol	*t*, °C	*n*-decyl alcohol	*t*, °C	*n*-undecyl alcohol	*t*, °C	*n*-dodecyl alcohol	*t*, °C	*n*-tridecyl alcohol	*t*, °C	*n*-tetradecyl alcohol
20	1222.3	20	1343.1	20	1397	20	1409	30	1389	40	1360	50	1335
30	1188.4	30	1309.6	30	1362	30	1375	40	1354	50	1326	60	1303
40	1149.7	40	1276.0	40	1327	40	1341	50	1320	60	1293	70	1270
50	1113.4	50	1243.4	50	1296	50	1307	60	1287	70	1260	80	1238
60	1075.1	60	1208.9	60	1259	60	1273	70	1254	80	1227	90	1206
70	1037.1	70	1157.9	70	1227	70	1239	80	1222	90	1195	100	1175
80	1000.5	80	1142.6	80	1193	80	1206	90	1191	100	1163	110	1143
90	961.6	90	1110.0	90	1160	90	1173	100	1159	110	1132	120	1112
100	923.4	100	1076.4	100	1128	100	1141	110	1127	120	1101	130	1081
110	884.7	110	1042.7	110	1095	110	1109	120	1096	130	1070	140	1049
120	845.1	120	1011.6	120	1063	120	1076	130	1064	140	1038	150	1018
130	804.4	130	977.6	130	1031	130	1045	140	1033	150	1007	160	988
140	764.2	140	943.8	140	999	140	1014	150	1001	160	976	170	957
150	723.3	150	909.3	150	966	150	982	160	971	170	945	180	927
160	681.9	160	875.3	160	933	160	950	170	940	180	915	190	897
170	639.4	170	839.3	170	901	170	918	180	910	190	884	200	866
180	597.5	180	804.1	180	867	180	885	190	879	200	854	210	836
190	554.5	190	768.7	190	835	190	853	200	849	210	824	220	806
200	510.6	200	732.9	200	803	200	821	210	818	220	794	230	777
210	466.4	210	696.7	210	769	210	789	220	787	230	765	240	747
220	420.5	220	660.1	220	736	220	758	230	757	240	736	250	719
230	371.6	230	623.4	230	703	230	726	240	726	250	707	260	690
240	317.5	240	587.2	240	671	240	696	250	696	260	678	270	661
250	255.2	250	550.5	250	638	250	665	260	666	270	649	280	633
260	179.3	260	512.8	260	607	260	634	270	637	280	621	290	604
265	133.3	270	476.1	270	576	270	603	280	608	290	592	300	576
		280	438.1	280	544	280	573	290	578	300	564	310	548
		290	399.7	290	512	290	543	300	549	310	536	320	520
		300	360.4	300	480	300	512	310	520	320	508	330	491
		310	319.9	310	448	310	480	320	491	330	480	340	467
		320	277.9	320	415	320	448	330	462	340	452	350	436
		330	233.4	330	382	330	416	340	432	350	424	360	405
				340	350	340	383	350	403	360	395	370	374
				350	317	350	350	360	373	370	366	380	342
				360	283	360	317	370	343	380	335	390	310
				370	250	370	283	380	310	390	305	400	278
				380	214	380	249	390	277	400	273	410	245
				390	181	390	214	400	243	410	239	420	211
				400	145	400	178	410	208	420	205	430	176
				410	107	410	141	420	171	430	169		
				420		420	103	430	132				
				430		430							

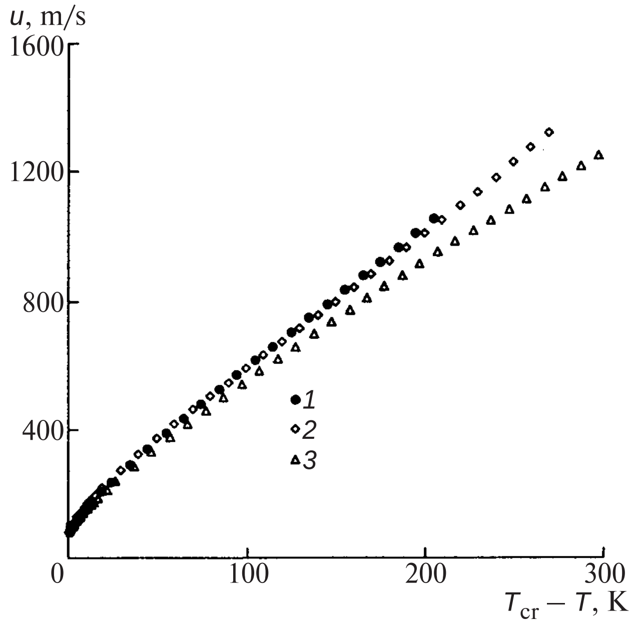

Fig. 6. A characteristic form of the temperature dependence of sound velocity in the investigated liquids on the saturation curve: (*1*) *n*-hexane, (*2*) benzene, (*3*) *n*-hexanol.

odal. Such a transition will be accompanied by the stratification of matter into phases existing in the form of suspension (thick mist). As a result, an expansion wave of low but finite amplitude will not propagate in this region. If the transmission of expansion waves of finite amplitude is in principle possible, their velocity is very low and will differ significantly from the velocity of compression waves. Therefore, signals from a harmonic source will have the form of a complex nonlinear wave in which the strong absorption of sound is caused by irreversible processes similar to those accompanying a shock wave.

The results of investigations performed at the KGU with numerous substances apparently support these conclusions. Indeed, at temperatures two or three degrees below the critical temperature, the absorption of ultrasonic waves is so significant that an ultrasonic pulse is fully absorbed by the medium at a distance of two or three millimeters from the radiator. As the critical point is approached, the increasing intensity of density fluctuations results in the emergence in the liquid of elastic periodic perturbations which are taken up by the receiving piezoelectric-crystal plate and seriously restrict the process of observation of the ultrasonic signal.

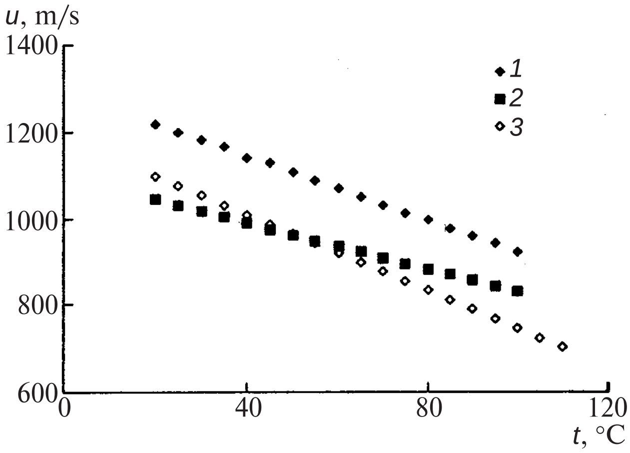

Fig. 7. The temperature dependence of sound velocity in (*1*) *n*-hexane, (*2*) 1-chlorohexane, and (*3*) 1-iodohexane.

Owing to the pulse-phase method used to measure the sound velocity, the critical point could be approached quite closely. As a result, the sound velocity could be recorded on almost the entire equilibrium curve in the liquid phase of a large number of substances including *n*-pentane, *n*-hexane, *n*-heptane, *n*-octane, *n*-nonane, benzene, toluene, diethyl ether, aliphatic alcohols, and other organic compounds [39, 40, 51, 52, 64]. In the vicinity of the critical point, the sound velocity was measured in vapor as well. The results obtained for saturated liquid are given in Tables 6–9, 14, 15, and 18, and those for vapor (saturated and superheated with $\rho \approx \rho_{cr}$ for $T > T_{cr}$) – in Tables 20–23.

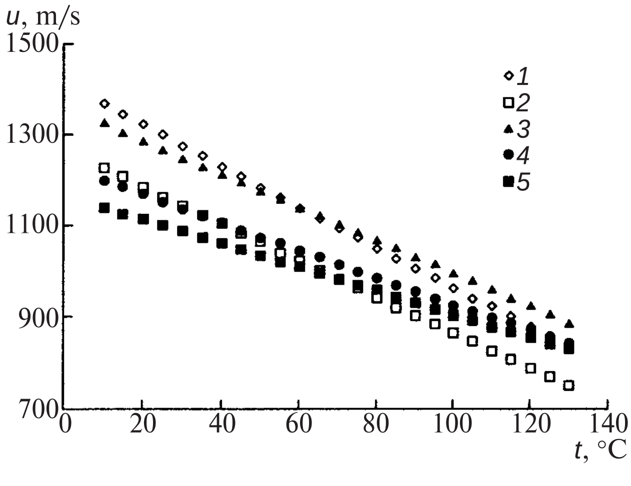

Fig. 8. The temperature dependence of sound velocity in (*1*) benzene and (*2*–*5*) its fluoro-, chloro-, bromo-, and iodo-compounds.

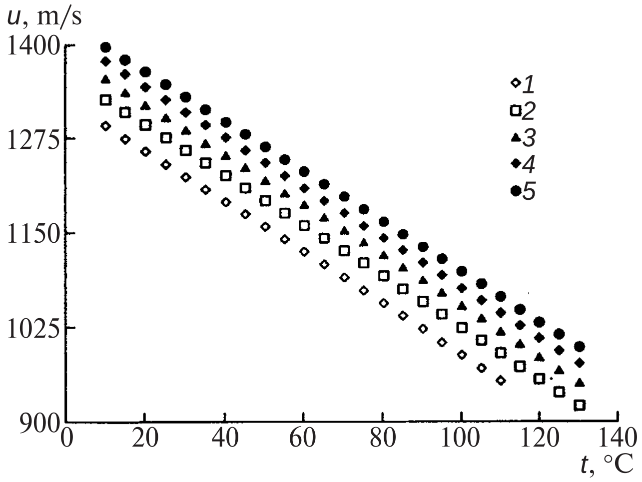

Fig. 9. The temperature dependence of sound velocity in normal aliphatic alcohols: (*1*) *n*-butanol, (*2*) *n*-pentanol, (*3*) *n*-hexanol, (*4*) *n*-heptanol, and (*5*) *n*-octanol.

When measuring the sound velocity in the vicinity of the critical point, it is very important to satisfy the condition of critical filling defined by the relation

$$V = (\rho_{cr}/\rho)V_0.$$

Here, V and ρ denotethe volume and density of the liquid being investigated at the temperature of filling of the autoclave, respectively; ρ_{cr} is its critical density; and V_0 is the volume of the interior of the autoclave. The error within which the condition of critical filling was valid was 0.3%.

Figure 13 gives the polytherms of the sound velocity in the liquid phase and in saturated and superheated vapors of *n*-hexane. A similar form of the $u(T)$ curves was observed for other substances as well. It follows from Fig. 13 that, as the temperature rises, the sound velocity in saturated liquid decreases by the nonlinear law. The temperature coefficient of sound velocity in the vicinity of the critical point increases rapidly to reach values which are two or three times that at room temperature. In saturated vapor in the investigated temperature range, the sound velocity likewise decreases with temperature. However, the temperature coefficient of sound velocity in vapor is low even in the vicinity of the critical point and is three or four times lower than that in liquid. At $T > T_{cr}$, the sound velocity in vapor whose density is close to critical increases with temperature. As a result, two or three kelvins before the critical point in saturated liquid and vapor one can observe low but finite values of sound velocity.

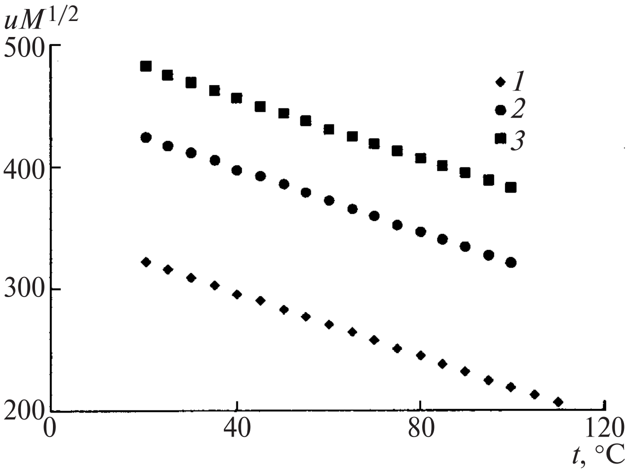

Fig. 10. Comparison of the molar velocities of sound of (*1*) *n*-hexane, (*2*) 1-chlorohexane, and (*3*) 1-iodohexane.

Analysis of the experimental results, performed within the known concepts of corresponding states, leads one to conclude that, in the region adjoining the critical point, the corresponding states for the sound velocity in the substances being investigated are realized at equal values of the difference $T_{cr} - T$. In so doing, the relation

$$u_1\sqrt{M_1} = u_2\sqrt{M_2} \qquad (10)$$

is valid. Here, M_1 and M_2 are the molar masses of homologs. Relation (10) is valid within individual homologous groups as well, for example, for monatomic aliphatic alcohols and *n*-alkanes. For the liquid phase of *n*-alkanes, it is valid in a wider temperature

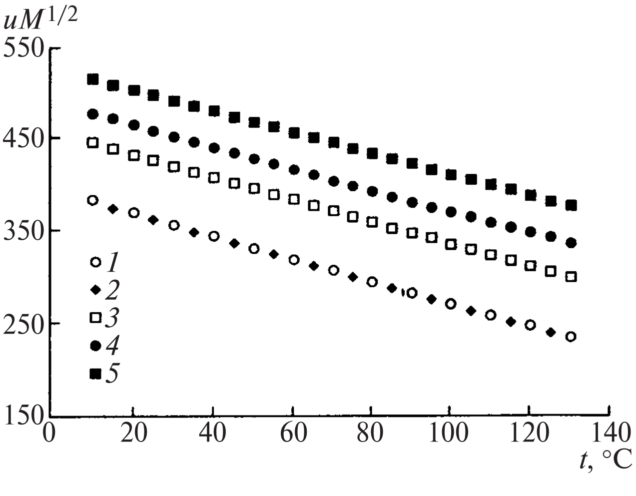

Fig. 11. Comparison of the molar velocities of sound of (*1*) benzene and (*2*–*5*) its fluoro-, chloro-, bromo-, and iodo-compounds.

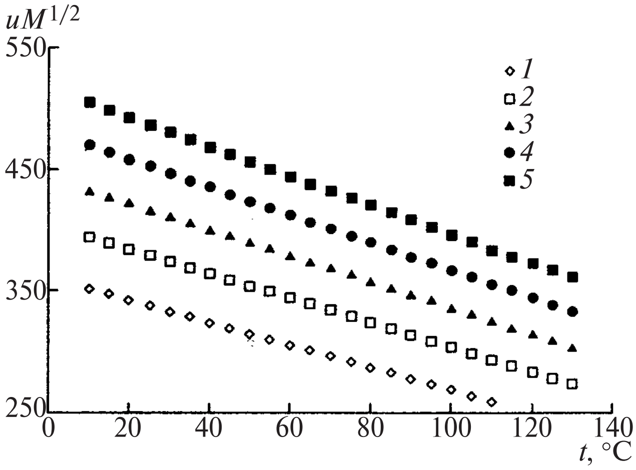

Fig. 12. Comparison of the molar velocities of sound of normal aliphatic alcohols: (*1–5*) see Fig. 9.

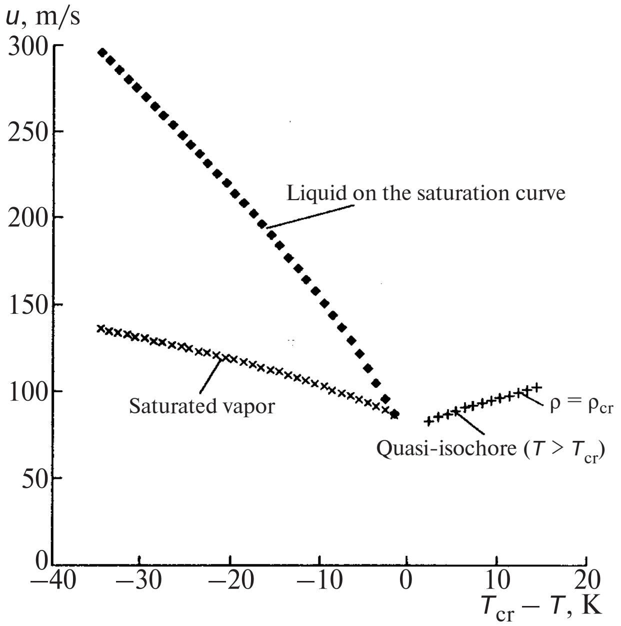

Fig. 13. The sound velocity in *n*-hexane in the vicinity of the critical point.

range as well. In the case of saturated and superheated vapor, relation (10) is approximate. Figure 14 illustrates the validity of regularity (10) for *n*-alkanes in the region adjacent to the critical point.

Experimentally obtained values of sound velocity along with the available data on the density of liquid and vapor [38, 126, 127] were used to estimate the adiabatic compressibility of both phases of investigated substances. Given in Fig. 15 by way of example are polytherms of the adiabatic compressibility of *n*-hexane.

It follows from the $\beta_S(T)$ curves that the adiabatic compressibility in the liquid phase increases abruptly on approaching the critical point, while the compressibility of saturated vapor first decreases slowly and, after passing a rather flat minimum, begins to slowly increase on approaching the critical point. The behavior of adiabatic compressibility depends on the accuracy of the available data on vapor density. The vapor density data given in [38, 126, 127] somewhat differ from one another. However, their differences have no significant effect on the general pattern of the temperature dependence of β_S. The adiabatic compressibility of a material of critical density increases markedly on approaching the critical point from the side of higher temperatures. It is obvious that the adiabatic compressibility must be expected to abruptly increase and tend to infinity in the immediate vicinity of the critical point.

One can see that the pulse-phase method of measuring the sound velocity employed by us at a frequency of 1 MHz failed to provide for approaching the critical point closer than by two or three degrees. In the case of *n*-alkanes, the width of the uninvestigated region increased with the number of the homolog.

4. DETERMINATION OF THE THERMODYNAMIC PROPERTIES OF LIQUID USING THE DATA ON ULTRASONIC VELOCITY

As was mentioned above, it is of great interest to investigate the properties of liquids on the saturation curve, because this enables one to obtain information about the individual properties of a substance by the experimental data on density, vapor pressure, heat capacity, and sound velocity in a wide range of parameters of state using rigorous thermodynamic relations. However, analysis of available results indicates that the work aimed at obtaining reliable consistent experimental data on the caloric and elastic properties of organic liquids is far from being completed. In particular, the data on the caloric properties of *n*-alkanes, given in [128] and [38, 126], lack consistency. Also inconsistent are the data of different researchers on isothermal compressibility, heat capacity ratio, and the temperature behavior of isochoric heat capacity of these substances on the saturation curve [38, 126–129]. The value of differences exceeds appreciably the value of errors specified in these papers. For example, the values of isobaric heat capacity of liquid *n*-hexane on the saturation curve at temperatures close

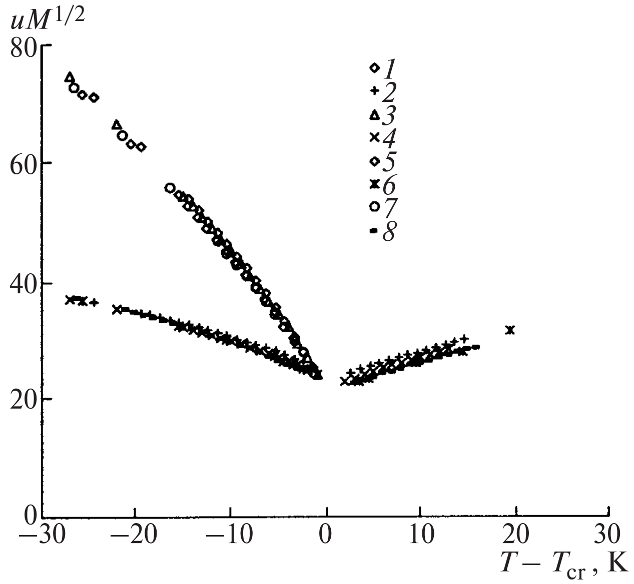

Fig. 14. An illustration of the law of corresponding states for the molar velocity of *n*-alkanes in the vicinity of the critical point: (*1*) *n*-hexane, (*2*) *n*-hexane vapor, (*3*) *n*-heptane, (*4*) *n*-heptane vapor, (*5*) *n*-octane, (*6*) *n*-octane vapor, (*7*) *n*-nonane, (*8*) *n*-nonane vapor.

to critical, recommended by the authors of [38, 126], diverge significantly and, at a temperature of 234°C differ from each other by a factor of almost four. This is especially unacceptable because *n*-hexane is often used as reference liquid.

We include the heat capacities Δc_V, c_V^{tph}, or c_s and derive a number of relations for thermodynamic calculations, which differ from one another significantly by their structures,

$$\gamma^2 \frac{T}{c_P}\left(\frac{1}{\rho u}\frac{dp_s}{dT}\right)^2 + \gamma\left(\frac{2\alpha_s T dp_s}{\rho c_P\, dT} - 1\right) + \left(\frac{\alpha_s^2 u^2 T}{c_P} - 1\right) = 0, \tag{11}$$

$$\gamma = \frac{c_s + u^2\alpha_s^2 T + \dfrac{\alpha_s T dp_s}{\rho\ dT}}{c_s - \dfrac{\alpha_s T dp_s}{\rho\ dT} - T\left(\dfrac{1}{\rho u}\dfrac{dp_s}{dT}\right)^2}, \tag{12}$$

$$\gamma = \frac{c_V^{\text{tph}} + u^2\alpha_s^2 T + \dfrac{2\alpha_s T dp_s}{\rho\ dT}}{c_V^{\text{tph}} - T\left(\dfrac{1}{\rho u}\dfrac{dp_s}{dT}\right)^2}, \tag{13}$$

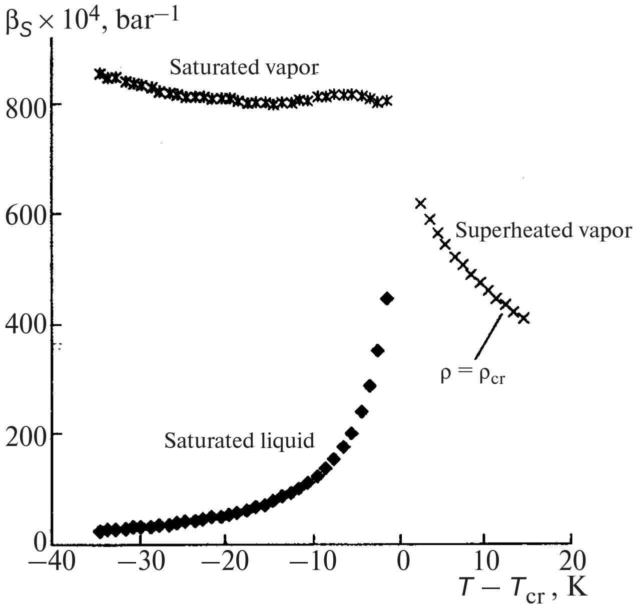

Fig. 15. The temperature dependence of adiabatic compressibility of *n*-hexane in the vicinity of the critical point.

$$\gamma^2\left[c_V - T\left(\frac{1}{\rho u}\frac{dp_s}{dT}\right)^2\right] - \gamma\left(c_V + \frac{2\alpha_s T dp_s}{\rho\ dT}\right) - u^2\alpha_s^2 T = 0, \tag{14}$$

$$\gamma = \frac{u^2\alpha_s^2 T}{\Delta c_V}. \tag{15}$$

The thermodynamic quantities which are present in relations (12)–(15) relate to one of the phases of matter. In the case of the liquid phase, $c_s = c'_s$ is the specific heat capacity of liquid on the saturation curve; $c_P = c'_P$; $c_V = c'_V$; $c_V^{\text{tph}} = c_V^{\text{tph}\prime}$ is the limiting value of specific two-phase heat capacity at constant volume (on condition that the volume occupied by the vapor phase $V'' \to 0$); and Δc_V is the jump of heat capacity [128] defined by the relation

$$\Delta c_V = c_V^{\text{tph}\prime} - c'_V.$$

The specific heat capacities $c_V^{\text{tph}\prime}$ and c'_s are closely related to each other [6],

$$c'_s = c_V^{\text{tph}\prime} + T\left(\frac{dp_s}{dT}\right)\left(\frac{dv'}{dT}\right)_S,$$

$$c'_s = c'_V + T\left(\frac{\partial p}{\partial T}\right)_V\left(\frac{dv'}{dT}\right)_s, \quad v' = \frac{1}{\rho'}.$$

Table 20. The sound velocity in C_6, C_7, C_9, C_{10} *n*-paraffins (vapor phase)

	u, m/s						
t, °C	*n*–hexane	*t*, °C	*n*–heptane	*t*, °C	*n*–nonane	*t*, °C	*n*–decane
160	163.9	190	153.8	260	133.4	270	137.3
165	161.9	195	151.5	265	129.7	275	134.7
170	158.9	200	148.9	270	126.4	280	131.9
175	155.7	205	145.9	275	122.0	285	128.4
180	152.5	210	142.9	280	118.2	290	125.2
185	148.9	215	139.5	285	114.2	295	121.5
190	145.1	220	135.9	290	109.4	300	117.4
195	140.6	225	132.0	295	104.3	305	113.1
200	135.8	230	127.7	300	99.0	310	108.7
205	130.6	235	122.6	301	97.4	315	102.8
210	124.7	240	117.3	302	95.9	320	97.1
215	118.1	245	111.4	303	94.6	325	90.4
216	116.9	250	104.9	304	93.4	330	83.6
217	115.7	251	103.4	305	92.0	331	82.0
218	114.2	252	102.0	306	90.7	332	80.4
219	112.6	253	100.6	307	89.2	333	78.8
220	111.2	254	99.0	308	87.8	334	77.3
221	109.5	255	97.4	309	86.2	335	75.4
222	108.0	256	95.8	310	84.8	336	74.1
223	106.3	257	94.2	311	83.2	337	71.9
224	104.7	258	92.5	312	81.6	338	70.3
225	102.9	259	90.8	313	79.9	339	68.3
226	101.1	260	89.0	314	78.0	340	66.5
227	99.4	261	87.5	315	75.8	341	–
228	97.5	262	85.4	316	73.9	342	–
229	95.6	263	83.5	317	71.7	343	–
230	93.6	264	81.3	318	69.7	t_{cr} = 344.5°C	
231	91.3	265	78.8	319	–	345	–
232	89.1	266	76.1	320	–	346	–
233	86.5	t_{cr} = 267.0°C		t_{cr} = 321.5°C		347	–
t_{cr} = 234.5°C		268	–	322	–	348	–
235	–	269	72.4	323	–	349	–
236	–	270	74.3	324	63.5	350	–
237	83.1	271	76.0	325	64.9	351	65.3
238	85.2	272	78.0	326	66.3	352	66.3
239	87.0	273	79.6	327	67.7	353	67.3
240	88.6	274	81.1	328	68.9	354	68.7
241	90.4	275	82.6	329	70.2	355	69.5
242	91.8	276	84.0	330	71.8	356	71.1
243	93.3	277	85.6	331	73.0	357	72.2
244	94.7	278	86.9	332	73.9	358	72.8
245	96.3	279	88.2	333	75.6	359	74.0
246	97.7	280	89.6	334	76.8	360	75.1
247	99.1			335	77.9	361	76.1
248	100.6			336	79.2	362	77.3

Table 21. The sound velocity in aromatic hydrocarbons (vapor phase)

u, m/s							
t, °C	benzene	t, °C	benzene	t, °C	toluene	t, °C	toluene
210	180.8	282	116.5	230	171.4	312	103.3
215	178.3	283	115.1	235	169.2	313	101.6
220	175.6	284	113.8	240	167.0	314	99.9
225	172.7	285	111.9	245	164.5	315	98.0
230	169.8	286	109.8	250	161.7	316	96.0
235	166.3	287	108.2	255	158.8	317	93.6
240	162.7	288	103.8	260	155.8	318	90.4
245	158.7	t_{cr} = 288.9°C		265	152.4	t_{cr} = 318.6°C	
250	154.6	290	103.8	270	148.0	320	–
255	148.1	291	105.4	275	144.7	321	–
260	145.3	292	106.8	280	140.7	322	89.9
265	139.5	293	108.1	285	136.1	323	91.0
270	133.6	294	109.3	290	131.2	324	92.8
271	132.1	295	110.5	295	125.6	325	94.1
272	130.9	296	111.7	300	119.6	326	95.1
273	129.6	297	112.8	301	118.5	327	96.4
274	128.2	298	114.0	302	117.2	328	97.4
275	126.9	299	115.1	303	116.1	329	98.2
276	125.5	300	116.2	304	114.8	330	99.9
277	124.1	301	117.3	305	113.5	331	101.0
278	122.7	302	118.5	306	112.2	332	102.2
279	121.2	303	119.6	307	110.8	333	103.0
280	119.8	304	120.8	308	109.5	334	104.1
281	118.2	305	121.6	309	108.0	335	105.2
				310	106.5	336	106.4
				311	105.0		

Here, υ' and ρ' denote the specific volume and density of saturated liquid.

The foregoing set of thermodynamic relations (11)–(15) and the experimental data on sound velocity are used to correlate the available data on the caloric and elastic properties of liquids and estimate their most probable values. It is convenient to start this process with the calculation of the ratio of heat capacities γ. In the presence of reliable input data, relations (11)–(15) must lead to the same results. This is confirmed by the calculation results. Note that relations (11)–(15) differ by their structures; therefore, they differ by their sensitivity to the inaccuracy of input experimental data. This sensitivity depends significantly on the region of the equilibrium curve in which the calculation relation is used. In view of this, formula (11), which is convenient for the calculation of γ on almost the entire equilibrium curve, turns out to be excessively sensitive to the inaccuracy of input experimental data in the region adjoining the critical point. Therefore, 5–7 °C before the critical point, this formula is of little use in thermodynamic calculations. In this region of states, relation (11) may be used as a highly sensitive indicator of consistency and reliability of the available data on the elastic and caloric properties of a substance. Most convenient for the calculation of γ in the foregoing temperature region are formulas (12)–(15) in which the heat capacities c_V, $c_V^{\text{tph}\prime}$, Δc_V, or c_s appear.

As a result of analysis of the available experimental data on the thermal properties of n-hexane on the liquid-vapor equilibrium curve, one can make sure that the data on saturated vapor pressure given in reference books [126, 127, 130], in papers [131, 132], and the data according to NIST [38] agree well with

Table 22. The sound velocity in aromatic hydrocarbons (vapor phase)

u, m/s											
t, °C	m-xylene	t, °C	m-xylene	t, °C	n-xylene	t, °C	n-xylene	t, °C	o-xylene	t, °C	o-xylene
230	169.0	336	95.6	245	164.3	336	93.6	260	163.9	349	93.1
235	167.4	337	94.1	250	162.4	337	91.9	265	162.0	350	91.4
240	166.1	338	92.4	255	160.5	338	90.1	270	159.9	351	89.5
245	164.5	339	90.6	260	158.2	339	88.2	275	157.6	352	87.4
250	162.6	340	88.7	265	156.0	340	86.2	280	155.1	353	85.7
255	160.5	341	86.8	270	153.5	341	84.0	285	152.6	354	83.7
260	158.4	342	84.7	275	150.7	342	81.6	290	149.8	355	81.1
265	156.2	343	82.1	280	148.0	t_{cr} = 343.0°C		295	147.0	t_{cr} = 356.8°C	
270	153.9	t_{cr} = 343.9°C		285	144.7	344	-	300	143.7	357	-
275	151.3	345	-	290	141.4	345	-	305	140.3	358	-
280	148.4	346	79.1	295	138.1	346	78.6	310	136.7	359	79.4
285	145.2	347	80.7	300	134.0	347	80.2	315	132.6	360	80.9
290	141.9	348	81.9	305	130.1	348	81.6	320	127.9	361	82.0
295	138.5	349	83.1	310	125.2	349	82.7	325	123.0	362	83.1
300	135.2	350	84.0	315	120.2	350	83.6	330	117.9	363	84.2
305	131.1	351	85.0	320	115.1	351	85.4	335	112.3	364	85.4
310	126.4	352	86.2	325	109.1	352	86.6	340	106.1	365	86.5
315	121.6	353	87.7	330	102.6	353	87.8	345	99.2	366	87.8
320	116.5	354	89.1	331	101.2	354	88.8	346	97.7	367	88.9
325	110.7	355	90.2	332	99.8	355	89.9	347	96.5	368	89.6
330	104.6	356	91.1	333	98.3	356	91.3	348	94.8		
331	103.1	357	92.3	334	96.8	357	92.5				
332	101.6	358	93.2	335	95.2	358	93.3				
333	100.2	359	94.6								
334	98.8	360	95.6								
335	97.2										

one another. These data provide for a high accuracy of the derivative dp_s/dT which appears in relations (11)–(15). In order to calculate the derivative dp_s/dT, we used the data on the pressure of saturated vapors of n-hexane recommended in [38]. This enabled us to calculate dp_s/dT with an error of 0.5% or less on almost the entire equilibrium curve except for the region adjoining the critical point, in which the error may reach 1–2%.

The experimental data on isobaric heat capacity c_P of liquid n-hexane at temperatures away from the critical point, given in [38, 126, 127, 132, 133], agree well with one another within 2%. At temperatures close to critical, the error of the c_P data increases abruptly. Therefore, at temperatures above 150°C, we used in calculations the experimental data on two-phase heat capacity $c_V^{\mathrm{tph}\prime}$ of n-hexane borrowed from Amirkhanov *et al.* [128] who estimated the error of measurement at 2%.

The data on density of the liquid phase of n-hexane, given in [38, 126, 127], agree with one another within 0.1% up to almost 200°C and diverge appreciably in the region adjoining the critical point (Fig. 16). In view of this, we averaged the data on density of the liquid phase of n-hexane by different researchers [38, 126, 127, 130]. The thus obtained values of density were used to calculate the thermal expansion coefficient α_s with an error of 1–2%. The exception is provided by the region adjoining the critical point, where the indeterminacy of the values of density proper reaches 8%.

The error of the data on sound velocity in n-hexane, given by us in Table 6, increases from 0.1% at

Table 23. The sound velocity in aliphatic alcohols (vapor phase)

u, m/s											
t, °C	isoamyl alcohol	t, °C	isoamyl alcohol	t, °C	isobutyl alcohol	t, °C	isobutyl alcohol	t, °C	n–butyl alcohol	t, °C	n–butyl alcohol
190	201.9	294	115.8	205	188.3	268	121.1	220	188.9	283	121.1
195	200.3	295	114.1	210	185.2	269	119.0	225	185.0	284	119.0
200	198.0	296	112.8	215	182.0	270	116.6	230	181.2	285	116.9
205	195.5	297	111.1	220	178.3	271	114.0	235	177.5	286	114.5
210	193.1	298	109.4	225	174.3	272	111.1	240	173.8	287	111.3
215	190.7	299	107.5	230	169.9	273	107.1	245	169.5	288	107.2
220	188.7	300	105.4	235	165.6	t_{cr} = 274.7°C		250	164.8	t_{cr} = 289.8°C	
225	185.8	301	103.2	240	160.2	275	–	255	159.8	290	–
230	182.8	302	100.7	245	155.2	276	–	260	154.4	291	102.6
235	179.9	303	97.9	250	149.4	277	102.1	265	148.7	292	105.1
240	176.3	t_{cr} = 304.1°C		255	142.8	278	104.5	270	142.7	293	107.3
245	172.8	305	–	256	141.3	279	106.2	271	141.2	294	109.4
250	168.8	306	90.1	257	139.9	280	108.2	272	139.8	295	111.2
255	164.8	307	92.1	258	138.5	281	110.2	273	138.0	296	112.9
260	159.9	308	94.0	259	136.9	282	111.9	274	136.5	297	114.7
265	155.0	309	95.7	260	135.9	283	113.5	275	134.9	298	116.2
270	150.0	310	97.4	261	134.1	284	115.1	276	133.4	299	118.0
275	142.8	311	98.7	262	132.2	285	116.5	277	131.7	300	119.4
280	136.8	312	100.1	263	130.6	286	118.0	278	130.2	301	120.9
285	130.1	313	101.5	264	128.9	287	119.6	279	128.6	302	122.5
286	128.7	314	103.2	265	126.7	288	121.1	280	126.4	303	124.1
287	127.2	315	104.2	266	125.0	289	122.6	281	124.7	304	125.6
288	125.5	316	105.7	267	123.1	290	124.0	282	122.8	305	126.9
289	123.9	317	107.0								
290	122.3	318	108.3								
291	120.8	319	109.5								
292	119.2	320	110.7								
293	117.4	321	111.9								

room temperature to 1% in the vicinity of the critical point, which is ±1 m/s in magnitude for the entire investigated temperature region.

The data on density, saturated vapor pressure, heat capacities c_P and $c_V^{\text{tph}\prime}$, and sound velocity of n-hexane were used to calculate and correlate other thermodynamic quantities. The calculation procedure was as follows. First, the calculation of γ was performed using the data on isobaric c_P and isochoric c_V heat capacities, given in [38]. For this purpose, the foregoing quadratic equations (11) and (14) were solved. Away from the critical point, the results of calculations of γ by Eqs. (11) and (14) fully agree with each other and with the values of γ obtained directly by the data on c_P and c_V given in [38]. However, even at 10–15°C below the critical point, the values of γ differ appreciably from each other. In view of this, the experimental data on heat capacity $c_V^{\text{tph}\prime}$ from [128] were used to perform thermodynamic calculations for n-hexane at temperatures above 150 °C. The heat capacity ratio in this case was determined by formula (13). The isochoric and isobaric heat capacities were calculated by the following relations:

$$c_V = c_V^{\text{tph}\prime} - \Delta c_V, \quad \Delta c_V = \frac{\alpha_s^2 u^2 T}{\gamma}, \quad c_P = \gamma c_V.$$

Analysis of the obtained results leads one to conclude that the values of γ obtained using the data on

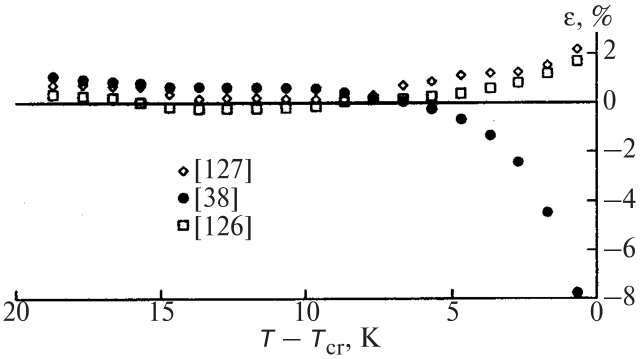

Fig. 16. The relative deviation of the data on density of the liquid phase of *n*-hexane, given in [38, 126, 127], relative to the values given in Table 24.

isochoric heat capacity $c_V^{tph\prime}$ are characterized by the highest reliability at high temperatures in the region adjoining the critical point. This is associated first of all with the mathematical singularities of relation (13) in which the errors of measurement of the heat capacity $c_V^{tph\prime}$ proper are partly compensated for and with the special features of the temperature dependence of $c_V^{tph\prime}$ which is a slowly increasing function of temperature, the pattern of whose variation changes significantly only in the immediate vicinity of the critical point.

Figure 17 gives curves of temperature dependence of isochoric heat capacity c_V of the liquid phase of *n*-hexane plotted by the data of [38] and calculated using the experimentally obtained values of c_P [38, 127, 132, 133] and $c_V^{tph\prime}$ [128], as well as by our data on sound velocity. A marked difference between the curves is observed only in the immediate vicinity of the critical point.

Given in Table 24 with due regard for the obtained results are the recommended values of the elastic and caloric properties of the liquid phase of *n*-hexane on the liquid-vapor equilibrium curve for temperatures from –80 to +234°C.

In Fig. 18 the values of isobaric heat capacity of liquid *n*-hexane for the region adjacent to the critical point obtained by us are compared to the values recommended in [38, 126]. One can see in Fig. 18 that a significant difference between the values of c_P is observed only in the vicinity of the critical point. The values of c_P obtained by us are approximately equally higher than the values recommended in [126] and

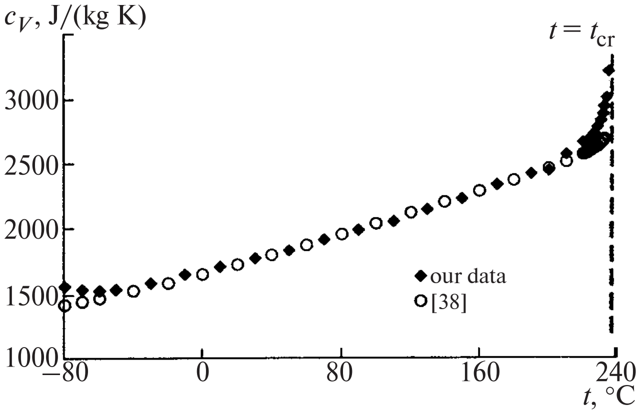

Fig. 17. The temperature dependence of specific isochoric heat capacity of the liquid phase of *n*-hexane on the saturation curve in the range from –80 to +234°C.

lower than the values of c_P given in [38]. We believe that the values calculated by us by the experimental data on two-phase heat capacity $c_V^{tph\prime}$ and sound velocity u measured on the saturation curve are more reliable in the region where appreciable differences between the values of c_P are observed. This is further confirmed by the consistency between the calculation results and the available input experimental results. For example, the ratios of heat capacity calculated by Eqs. (11), (13), and (14) to a temperature of 231°C completely coincide. A significant difference between the calculated values of γ, c_P, and others is observed only at temperatures of 233 and 234°C close to the critical point, apparently, because of the inaccuracy of the density data used in calculations. It follows from Fig. 16 that the difference in the density values [38, 128, 129] for the liquid phase of *n*-hexane in the temperature region being treated exceeds 8%.

Note that the data on the caloric and elastic properties of *n*-hexane for the equilibrium curve, given in [38, 128], were obtained by extrapolation to the saturation curve from the single-phase region. The pattern of such extrapolation is of critical importance. This is obvious from analysis of the results on the sound velocity in liquid *n*-hexane [38, 126], which differ significantly in the vicinity of the critical point from each other and from our experimentally obtained values (Table 25). The difference between these values in saturated vapor of *n*-hexane is small and amounts to ±1 m/s.

The experimental data on sound velocity and data on density, isobaric heat capacity, and saturated vapor

Table 24. The thermodynamic properties of the liquid phase of *n*-hexane on the saturation curve, calculated by the data on sound velocity (t_{cr} = 234.4°C)

t, °C	ρ, kg/m^3	$\alpha_S \times 10^3$, K^{-1}	dp_S/dT, Pa/K	c_P, J/(kg K)	c_V, J/(kg K)	c_V^{tph}, J/(kg K)	c_P/c_V	u, m/s	$\beta_T \times 10^{10}$, Pa^{-1}
–80	745.2	1.050	0.5	1981	1559		1.270	1586.0	6.78
–70	737.2	1.110	2.1	1991	1537		1.296	1534.0	7.47
–60	728.8	1.170	8.7	2007	1521		1.320	1483.0	8.23
–50	720.2	1.190	19	2029	1537		1.320	1433.0	8.92
–40	711.6	1.210	38	2054	1559		1.317	1382.0	9.69
–30	703.0	1.220	71	2082	1591		1.309	1333.0	10.48
–20	694.5	1.230	125	2113	1619		1.305	1296.0	11.18
–10	685.9	1.260	209	2145	1651		1.299	1239.0	12.34
0	677.2	1.280	332	2177	1685		1.292	1191.0	13.45
10	668.5	1.315	506	2209	1712		1.290	1148.0	14.64
20	659.6	1.360	743	2240	1733		1.293	1098.6	16.24
30	650.6	1.410	1055	2290	1770		1.293	1054.4	17.88
40	641.3	1.460	1456	2340	1811		1.292	1010.2	19.75
50	631.8	1.520	1957	2385	1843		1.294	965.7	21.96
60	622.1	1.590	2570	2431	1875		1.296	921.1	24.56
70	612.1	1.650	3306	2478	1914		1.295	877.9	27.44
80	601.8	1.730	4176	2526	1948		1.296	833.8	30.96
90	591.3	1.800	5186	2572	1985		1.292	789.8	35.03
100	580.7	1.890	6351	2621	2022		1.292	746.9	39.89
110	569.3	1.990	7675	2671	2062		1.292	704.1	45.79
120	557.8	2.10	9163	2720	2105		1.291	659.5	53.20
130	545.9	2.24	10828	2780	2150		1.293	616.0	62.42
140	533.4	2.41	12676	2840	2190		1.299	573.2	74.13
150	520.1	2.61	14694	2886	2205	2822	1.309	529.4	89.80
160	506.2	2.83	16941	2966	2260	2881	1.312	484.8	110.3
170	491.5	3.14	19415	3067	2315	2952	1.324	439.3	139.6
180	475.2	3.60	22140	3171	2340	3010	1.355	393.0	184.6
190	457.0	4.30	25150	3334	2371	3098	1.406	345.4	257.9
200	435.5	5.36	28500	3573	2407	3207	1.485	295.6	390.1
210	410.0	6.63	32300	3933	2542	3349	1.547	242.5	641.7
220	379.6	9.84	36700	4684	2604	3500	1.799	183.7	1404
222	371.9	11.0	37650	5028	2668	3598	1.884	171.0	1730
224	363.2	12.7	38650	5464	2687	3663	2.033	157.7	2250
226	353.5	14.6	39700	6044	2743	3739	2.203	143.8	3010
228	342.6	17.7	40800	7010	2784	3827	2.518	129.3	4395
230	329.1	23.6	41800	8990	2813	3927	3.194	112.7	7640
231	320.8	27.9	42350	10750	2877	4020	3.736	104.3	10710
232	311.2	34.2	42891	13740	2970	4132	4.64	95.4	16370
233	299.5	49	43000	21320	2990	4262	7.14	86.6	31790
234	282.2	79	43000	44500	3120	4459	14.3	77.7*	83700

*the value of sound velocity obtained by extrapolation

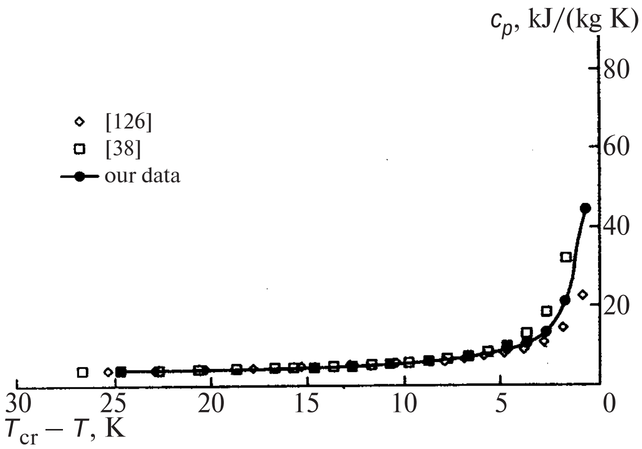

Fig. 18. The temperature dependence of isobaric compressibility of the liquid phase of *n*-hexane in the vicinity of the critical point.

pressure provide a reliable source of information about the value and pattern of temperature dependence of isochoric heat capacity of other liquids. Figure 19 gives the temperature dependences of molar isochoric heat capacity $C_V = f(T)$ for three classes of liquids investigated by us in the temperature range from 10 to 130°C.

It follows from analysis of the graphs of $C_V = f(T)$ that the substitution of a hydrogen atom by a halogen atom leads to an increase in C_V. The increase in C_V is the greater, the larger the mass of hydrogen-substituting halogen. This is apparently associated with the higher intensity of vibrations of the halogen atom in the C–Hal bond because of the increase in its mass and in the bond length. In addition, the increase in the mass of halogen leads to a marked disturbance of the molecular symmetry, which may cause the emergence of additional deformation vibration modes.

It follows further from the $C_V(T)$ graphs that the isochoric heat capacity increases most rapidly with temperature. Its increase is the slowest in aromatic compounds. One can see in Fig. 19 a tendency towards equalization of the temperature coefficients of isochoric heat capacity of investigated liquids in the region of higher temperatures.

Table 25. The values of sound velocity in the liquid phase of *n*-hexane in the vicinity of the critical point

t, °C	*u*, m/s		
	Our data	[38]	[126]
220	183.6	187.2	190.7
221	177.3	180.4	185.1
222	171.0	173.6	179.0
223	164.5	166.5	173.0
224	157.8	159.4	166.8
225	150.8	152.1	160.5
226	143.8	144.7	154.3
227	136.5	137.0	148.0
228	128.9	129.3	141.4
229	121.0	121.4	134.8
230	112.8	113.4	127.9
231	104.4	105.5	120.8
232	95.5	97.8	113.6
233	86.3	91.0	106.1
234	77.7	85.9	98

5. THE ULTRASONIC VELOCITY AND FLUCTUATIONS OF DENSITY. SATURATION CURVE AS A COMBINATION OF BASE STATES OF MATTER

The thermodynamic theory of fluctuations points to the correlation between the mean-square fluctuation of volume and the elastic properties of matter. This correlation is described by

$$\langle \Delta V^2 \rangle = kT\left(\left|\frac{\partial V}{\partial P}\right|\right)_T, \qquad (15)$$

where $\langle \Delta V^2 \rangle$ is the square of mean-square fluctuation of volume, and k is the Boltzmann constant.

One can compare the expressions for relative fluctuations of volume in ideal gas,

$$\left.\frac{\langle \Delta V^2 \rangle}{V^2}\right|_{\mathrm{G}} = \frac{1}{N}, \qquad (16)$$

where N is the number of particle in volume V, and for the respective condensed system under similar conditions,

$$\left.\frac{\langle \Delta V^2 \rangle}{V^2}\right|_{\mathrm{L}} = \frac{kT}{V}\beta_T, \qquad (17)$$

and derive the formula for isothermal compressibility of the condensed system

$$\frac{1}{\beta_T} = \nu\frac{RT}{M}\rho. \qquad (18)$$

Here, the dimensionless parameter ν is defined by the ratio of squares of relative fluctuations of volume in ideal gas and in the respective condensed system, R is the universal constant, and M is the molar mass of matter.

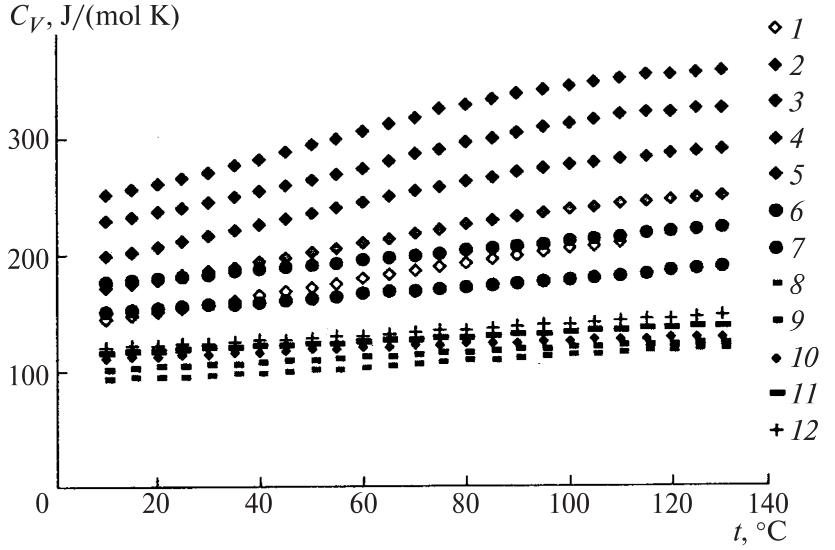

Fig. 19. Comparison of the molar isochoric heat capacities of the investigated liquids: (*1*) *n*-butanol, (*2*) *n*-pentanol, (*3*) *n*-hexanol, (*4*) *n*-heptanol, and (*5*) *n*-octanol, (*6*) *n*-hexane, (*7*) *n*-heptane, (*8*) benzene, (*9*) fluorobenzene, (*10*) chlorobenzene, (11) bromobenzene, (*12*) iodobenzene.

The following formula may be derived for the sound velocity in liquid using Eq. (18):

$$u^2 = \gamma\frac{RT}{M}\nu. \tag{19}$$

The dimensionless parameter ν appearing in this formula varies in a wide range from unity for ideal gas to several tens for liquid.

One can demonstrate within the classical statistical theory that the quantity ν is related to the integral of states Q

$$\nu = -\frac{V^2}{N}\left(\frac{\partial^2 \ln Q}{\partial V^2}\right)_T \tag{20}$$

and may be represented by two terms $\nu = 1 + \nu_{\text{int}}$, where ν_{int} is the term due to the interaction of particles.

The value of $\nu_{\text{int}} = \nu - 1$, defined by the pattern and intensity of intermolecular forces, will depend on the interparticle spacing and, in the end, on the liquid density.

A relation similar to Eq. (18) was obtained previously by Filippov [135, 136] who analyzed extensive empirical data and arrived at a conclusion of the existence of some “parachor” – a parameter similar to ν and characterized by the universal dependence on the liquid density ρ.

The data on sound velocity and heat capacity ratio, obtained by us, make it possible to estimate the parameter ν in a fairly wide temperature range for a large number of liquids. The estimation of the parameter ν leads one to conclude that, in a rather wide temperature region from T_{melt} to T_{boil}, the value of $\ln(\nu - 1)$ depends linearly on the liquid density ρ. This indicates that the dependence of ν on ρ may be represented by

$$\nu - 1 = (\nu_0 - 1)\exp(\alpha\Delta\rho), \tag{21}$$

where α is an individual empirical constant, and $\Delta\rho$ is the density difference for two arbitrary values of ν and ν_0.

As an example, Figs. 20–22 give the dependences of $\ln(\nu - 1)$ on ρ for the liquid phase of *n*-alkanes, *n*-alcohols, benzenes, and their binary mixtures.

The assumption that the pattern of the dependence of ν on ρ in the single-phase region will be the same as on the saturation curve makes it possible to derive a simple differential relation

$$\left(\frac{\partial p}{\partial \rho}\right)_T = \frac{RT}{M}\nu(\rho),$$

which is readily integrable in view of condition (21) and leads to the formula for the calculation of liquid density on the selected isotherm as a function of pressure,

$$\rho = \rho_0 + \frac{1}{\alpha}\ln\left(\frac{\alpha M\Delta p}{RT(\nu_0 - 1)}\left(1 - \frac{1}{\nu}\right) + 1\right). \tag{22}$$

Here, ρ_0 is the liquid density on the saturation curve, Δp is the pressure difference in the single-phase

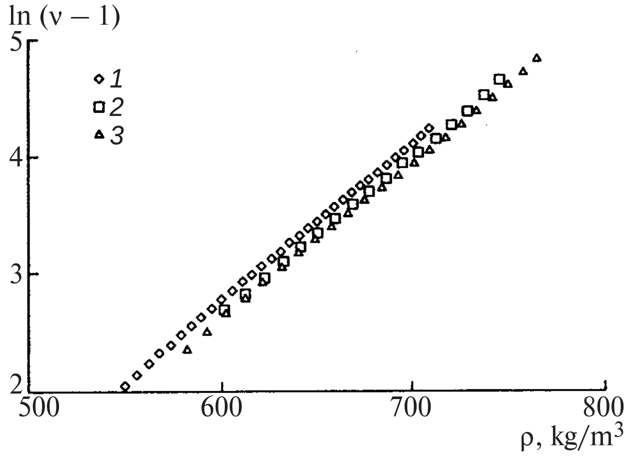

Fig. 20. The linear dependence of ln(ν – 1) on density for *n*-alkanes: (*1*) *n*-pentane, (*2*) *n*-hexane, (*3*) *n*-heptane.

region and on the boundary curve, ν_0 is the value of the parameter ν on the saturation curve, M is the molar mass of liquid, and α is a constant for the given liquid.

Tables 26 and 27 give the values of isothermal compressibility and density of liquid *n*-heptane, calculated by formulas (18) and (22).

A relation similar to formula (19) may be derived within the concepts of the "free" volume theory,

$$u^2 = \gamma\frac{RT}{M}\left(\frac{V}{V_f}\right)^{2/3}, \qquad (23)$$

where V_f is the free volume.

Comparison of formulas (19) and (23) leads one to quite a sound conclusion that the value of volume fluctuations is closely related to the value of "free" volume,

$$\nu = \left(\frac{V}{V_f}\right)^{2/3}. \qquad (24)$$

It follows from formula (24) that the observed increase in the parameter ν with increasing density of liquid is defined by the decrease in the "free" volume V_f.

The obtained results indicate that the states of liquid on the saturation curve must be treated as a combination of base states involved in the formation of the properties of liquid under different conditions. Such concepts enable one to search for an equation relating the thermodynamic parameters of liquid that would be convenient for theoretical analysis and adequately accurate for practical uses.

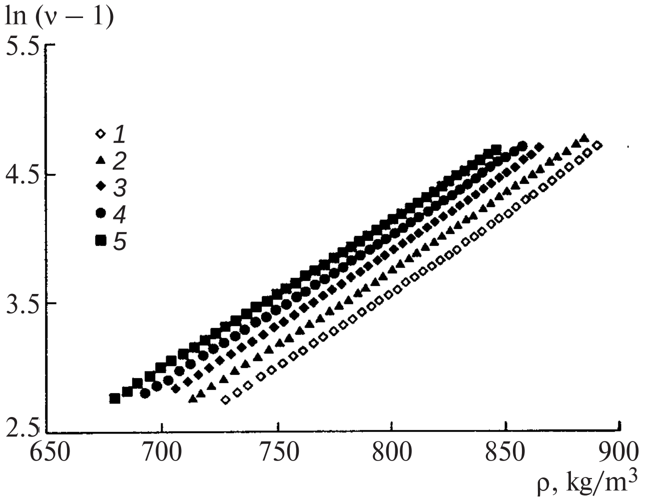

Fig. 21. The linear dependence of ln(ν – 1) on density for normal aliphatic alcohols: (*1*) *n*-butanol, (*2*) *n*-pentanol, (*3*) *n*-hexanol, (*4*) *n*-heptanol, and (*5*) *n*-octanol.

Such a relation which deserves attention is, for example, the differential equation relating the thermal coefficient of pressure to the interaction energy of particles of a condensed system,

$$T\left(\frac{\partial p}{\partial T}\right)_V = \frac{|E_P|}{v} + \frac{NkT}{v}, \qquad (25)$$

where $\left(\frac{\partial p}{\partial T}\right)_V$ is the thermal coefficient of pressure, and $|E_P|$ is the specific interaction energy of particles of the system. This relation may be validated within a simple discrete-continual model [139].

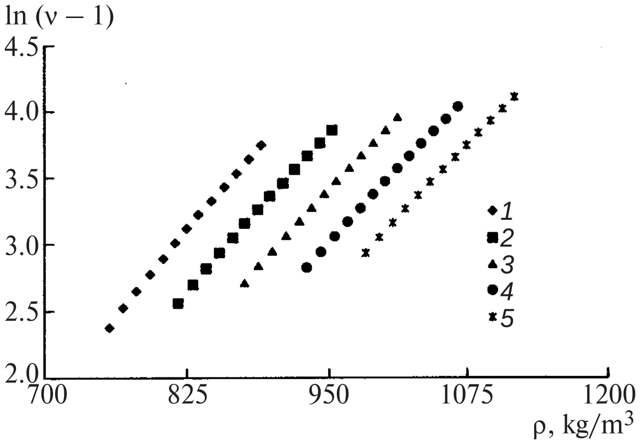

Fig. 22. The linear dependence of ln(ν – 1) on density benzene, chlorobenzene, and their binary mixture: (*1*) benzene 1.00, (*2*) benzene 0.75, (*3*) benzene 0.50, (*4*) benzene 0.25, and (*5*) chlorobenzene 1.00.

Table 26. Comparison of the calculated values of isothermal compressibility of *n*-heptane with experimental data

p, bar	$\beta_T \times 10^{10}$, Pa^{-1}					
	Calculation by Eq. (18)	[137, 138]	Calculation by Eq. (18)	[137, 138]	Calculation by Eq. (18)	[137, 138]
	t = 0 °C		t = 50 °C		t =100 °C	
0	119.3	119.4	180.9	181.1	301.1	302.7
50	112.4	116.2	165.9	174.6	265.3	262.4
100	106.3	107.8	154.1	156.0	237.2	220.1
200	95.5	96.3	135.1	132.9	197.9	185.3
300	86.8	87.5	117.3	117.0	169.2	156.8
500	72.8	74.6	99.0	95.3	130.9	121.3
1000	–	55.4	65.4	66.6	83.1	79.4

Table 27. Comparison of the calculated values of density of *n*-heptane with the data of Eduljee *et al.* [131]

p, bar	ρ, kg/m^3			ρ, kg/m^3		
	[131]	(22)	ε, %	[131]	(22)	ε, %
	t = 40 °C			t = 60 °C		
1	666.6	666.6	0.0	649.2	649.2	0.0
500	707.9	708.5	0.1	694.3	696.6	0.3
1000	735.8	735.2	0.1	724.3	725.4	0.1
1500	757.4	754.8	0.3	746.9	746.1	0.1
2000	775.3	770.3	0.6	765.5	762.3	0.2

Experimental data on density, heat capacity, saturated vapor pressure, and sound velocity enable one to calculate the thermal coefficient of pressure at any point of the equilibrium curve. This provides a possibility of estimating the interaction energy of liquid and vapor particles and study the pattern of its variation with temperature from the melting point to the critical point, including the critical point proper.

6. CONCLUSIONS

An objective of this review is to familiarize researchers involved in studies of the thermodynamic properties of liquids and their vapors with the extensive array of experimental data obtained at the Kursk State University on the sound velocity on the saturation curve in various organic substances, first of all, for saturated liquid. These data may be used to solve numerous diverse practical and theoretical problems. One such problem is to correlate the available experimental data on the elastic and caloric properties of liquids with subsequent detailed analysis of the thermodynamic surface and to construct the equation of state for a condensed system.

Another objective of the review is to familiarize researchers with the fairly simple, reliable, and precise method of measuring the sound velocity, developed at the Kursk State University.

In our opinion, further investigations of the thermodynamic properties of liquid on the saturation curve must be aimed at reducing the range of temperatures in the vicinity of the critical point which is still inaccessible for measurements of the sound velocity. Reliable experimental data on the elastic and caloric properties of matter in this region of states will make it possible to develop an adequate molecular-kinetic model explaining the singularities of the properties of matter in the critical region.

NOTATION

u, ultrasonic velocity; λ, wavelength; f, vibration frequency; ω, cyclic frequency; τ, relaxation time; τ_i, delay time of the ith pulse; L, acoustic path length; D, piezoradiator diameter; T, absolute temperature; T_{cr}, critical temperature in K; t, temperature on the Celsius scale; t_{cr}, critical temperature in °C; V, volume of a thermodynamic system; V_f, free volume; p, pressure;

p_s, saturated vapor pressure; ρ, density; ρ_{cr}, density of matter at the critical point; v, specific volume; c_v, specific isochoric heat capacity; c_P, specific isobaric heat capacity; c_s, specific heat capacity of liquid on the saturation curve; c_V^{tph}, limiting value of the specific two-phase heat capacity of liquid; Δc_V, specific value of a jump of heat capacity of liquid; C_V, molar isochoric heat capacity; β, thermal coefficient of linear expansion; α_p, isobaric thermal coefficient of volume expansion; α_s, thermal coefficient of volume expansion on the saturation curve; β_T, isothermal compressibility of liquid; β_S, adiabatic compressibility of liquid; R, universal gas constant; k, Boltzmann constant; M, molar mass; ε, relative error; $\left(\frac{\partial p}{\partial T}\right)_V$, isochoric thermal coefficient of pressure; dp_s/dT, thermal coefficient of saturated vapor pressure; $|E_P|$, specific energy of intermolecular interaction; ν, ratio of squares of relative fluctuations of volume of ideal gas and respective liquid; the symbol $'$ relates a physical quantity to saturated liquid; and the symbol $''$ relates a physical quantity to saturated vapor.

REFERENCES

1. Mikhailov, I.G., Solov'ev, V.A., and Syrnikov, Yu.P., *Osnovy molekulyarnoi akustiki* (Fundamentals of Molecular Acoustics), Moscow: Nauka, 1964.
2. *Physical Acoustics*, Mason, W.P., Ed., vol. 2, part A, New York: Academic Press, 1965. Translated under the title *Svoistva gazov, zhidkostei i rastvorov. Fizicheskaya akustika*, Moscow: Mir, 1968.
3. Friend, D.G., *Exp. Methods Phys. Sci.*, 2001, vol. 39, p. 237.
4. Vukalovich, M.P. and Novikov, I.I., *Termodinamika* (Thermodynamics), Moscow: Mashinostroenie, 1972.
5. Baidakov, V.G. and Skripov, V.P., *Zh. Eksp. Teor. Fiz.*, 1978, vol. 75, issue 3(9), p. 1007.
6. Oakley, B.A., Barber, G., Worden, T., and Hanna, D., *J. Phys. Chem. Ref. Data,* 2003, vol. 32, p. 1501.
7. Nozdrev, V.F., *Primenenie ul'traakustiki v molekulyarnoi fizike* (The Uses of Ultrasonics in Molecular Physics), Moscow: GIFML, 1958.
8. Kolesnikov, A.K., *Ul'trazvukovye izmereniya* (Ultrasonic measurements), Moscow: Izd. Standartov, 1982.
9. Ewing, M.B., Goodwin, A.R.H., McGlashan, M.L., and Trusler, J.P.M., *J. Chem. Thermodyn.*, 1987, vol. 19, p. 721.
10. Aleksandrov, A.A. and Larkin, D.K., *Teploenergetika*, 1977, no. 1, p. 73.
11. *Physics of Simple Liquids*, Temperley, H.N.V., Rowlinson, J., and Rushbrooke, G.S., Eds., Amsterdam: North-Holland, 1968. Translated under the title *Fizika prostykh zhidkostei. Eksperimental'nye issledovaniya*, Moscow: Mir, 1973.
12. Belogol'skii, V.A., Sekoyan, S.S., Samorukova, L.M. *et al.*, *Izmer. Tekh.*, 1999, no. 4, p. 66.
13. Simonsohn, G. and Wagner, F., *J. Phys. D*, 1989, vol. 22, p. 1179.
14. Boelhouwer, I.W.H., *Physica*, 1967, vol. 34, p. 484.
15. Kling, R., Nicolini, E., and Tissot, J., *Rech. Aeronaut.*, 1953, vol. 31, p. 31.
16. Takagi, T., *Rev. High Pressure Sci. Tech.*, 1994, vol. 3, p. 311.
17. Trusler, J.P.M., *Int. J. Thermophys.*, 1997, vol. 18, p. 635.
18. Moldover, M.R., Trusler, J.P.M., Edwards, T.J. *et al.*, *Phys. Rev. Lett.*, 1988, vol. 60, p. 249.
19. Khasanshin, T.S. and Shchemelev, A.P., *Teplofiz. Vys. Temp.*, 2001, vol. 39, no. 1, p. 64 (*High Temp.* (Engl. transl.), vol. 39, no. 1, p. 60).
20. Ewing, M.B., Goodwin, A.R.H., McGlashan, M.L., and Trusler, J.P.M., *J. Chem. Thermodyn.*, 1988, vol. 20, p. 243.
21. Ewing, M.B., Goodwin, A.R.H., and Trusler, J.P.M., *J. Chem. Thermodyn.*, 1989, vol. 21, p. 867.
22. Estrada-Alexanders, A.F., Trusler, J.P.M., and Zarari, M.P., *Int. J. Thermophys.*, 1995, vol. 16, p. 663.
23. Estrada-Alexanders, and Justo, D., *J. Chem. Thermodyn.*, 2004, vol. 36, p. 419.
24. Takagi, T., *J. Chem. Eng. Data*, 1996, vol. 41, p. 1325.
25. Takagi, T., *Curr. Jpn. Mater. Res.*, 1994, vol. 13, p. 169.
26. Takagi, T., Kusunoki, M., and Hongo, M., *J. Chem. Eng. Data*, 1992, vol. 37, p. 39.
27. Takagi, T., *J. Chem. Eng. Data*, 1991, vol. 36, p. 394.
28. Takagi, T. and Teranishi, H., *J. Chem. Eng. Data*, 1988, vol. 33, p. 169.
29. Dutour, S., Lagourette, B., and Daridon, J.L., *J. Chem. Thermodyn.*, 2002, vol. 34, p. 475.
30. Dutour, S., Daridon, J.L., and Lagourette, B., *High Temp. High Pressures*, 2001, vol. 33, p. 371.
31. Dutour, S., Daridon, J.L., and Lagourette, B., *J. Chem. Thermodyn.*, 2001, vol. 33, p. 765.
32. Daridon, J.L. and Lagourette, B., *High Temp. High Pressures*, 2000, vol. 32, p. 83.
33. Dutour, S., Daridon, J.L., and Lagourette, B., *J. Chem. Thermodyn.*, 2000, vol. 21, p. 173.
34. Trusler, J.P.M. and Zarari, M, *J. Chem. Thermodyn.*, 1992, vol. 24, p. 973.
35. Estrada-Alexanders, A.F. and Trusler, J.P.M., *J. Chem. Thermodyn.*, 1997, vol. 29, p. 991.
36. Trusler, J.P.M. and Zarari, M, *J. Chem. Thermodyn.*, 1996, vol. 28, p. 329.
37. Ball, S.J. and Trusler, J.P.M., *Int. J. Thermophys.*, 2001, vol. 22, p. 427.
38. http//webbook.nist.gov.
39. Neruchev, Yu.A., The Elastic Properties and Molecular Structure of *n*-Paraffins on the Saturation Curve, *Cand. Sci. (Phys.-Math.) Dissertation*, Kursk: KGPI (Kursk State Pedagogical Inst.), 1970.

40. Zotov, V.V., Investigation of the Equilibrium Properties of Alkyl Benzenes and Aliphatic Alcohols on the Saturation Curve Using the Acoustic Method, *Cand. Sci. (Phys.-Math.) Dissertation,* Kursk: KGPI (Kursk State Pedagogical Inst.), 1972.
41. Melikhov, Yu.F., Acoustic Investigations of the Equilibrium Properties and the Equation of State of Polyatomic Liquids at High Pressures, *Cand. Sci. (Phys.-Math.) Dissertation*, Kursk: KGPI (Kursk State Pedagogical Inst.), 1984.
42. Mel'nikov, G.A., The Acoustic Properties, Viscosity, and Structure of a Number of Organic Liquids, *Cand. Sci. (Phys.-Math.) Dissertation,* Kursk: KGPI (Kursk State Pedagogical Inst.), 1989.
43. Merkulov, A.G. and Tret'yakov, V.G., *Akust. Zh.*, 1974, vol. 20, issue 4, p. 596.
44. Gitis, M.B. and Khimunin, A.S., *Akust. Zh.*, 1968, vol. 14, issue 4, p. 489.
45. Kononenko, V.S., *Akust. Zh.*, 1974, vol. 20, issue 2, p. 269.
46. Carome, E.F., Witting, I.M., and Flenry, P.A., *J. Acoust. Soc. Am.*, 1961, vol. 33, no. 10, p. 1417.
47. Burundukov, K.M. and Lobanov, A.M., *Akust. Zh.*, 1970, vol. 16, issue 5, p. 776.
48. Okhotin, V.S., Razumeichenko, L.A., Kas'yanov, Yu.I., and Skorodumov, A.V., *Teplofizich. Svoistva Veshchestv Mater.*, 1986, issue 23, p. 5.
49. Will, S., Froba, A.P., and Leipertz, A., Thermal Diffusivity and Sound Velocity of Toluene over a Wide Temperature Range, *Thirteenth Symp. on Thermophysical Properties*, Boulder, Col., 1997 (http://symp14.nist.gov).
50. Novikov, I.I. and Sheludyakov, E.P., *Prikl. Mekh. Tekh. Fiz.*, 1964, no. 6, p. 119.
51. Zotov, V.V., Melikhov, Yu.F., Mel'nikov, G.A., and Neruchev, Yu.A., *Skorost' zvuka v zhidkikh uglevodorodakh* (The Sound Velocity in Liquid Hydrocarbons), Kursk: KGPU (Kursk State Pedagogical Univ.), 1995.
52. Zotov, V.V., Neruchev, Yu.A., and Otpushchennikov, N.F., Experimental Investigation of the Sound Velocity in Some Organic Liquids, in *Ul'trazvuk i fiziko-khimicheskie svoistva veshchestva* (Ultrasound and the Physicochemical Properties of Matter), Kursk: Izd. KGPI (Kursk State Pedagogical Inst.), 1969, p. 25.
53. Zotov, V.V. and Neruchev, Yu.A., Approximate Calculation of the Thermodynamic Properties of Toluene and *m*-Xylene on the Saturation Line, in *Ul'trazvuk i fiziko-khimicheskie svoistva veshchestva* (Ultrasound and the Physicochemical Properties of Matter), Kursk: Izd. KGPI (Kursk State Pedagogical Inst.), 1969, p. 42.
54. Pishchikov, I.M. and Sobolev, V.D., The Velocity and Absorption of Sound in Diphenyl Ether, in *Ul'trazvuk i fiziko-khimicheskie svoistva veshchestva* (Ultrasound and the Physicochemical Properties of Matter), Kursk: Izd. KGPI (Kursk State Pedagogical Inst.), 1969, p. 47.
55. Zotov, V.V., Experimental Investigation of the Sound Velocity in Vapors of Monatomic Aliphatic Alcohols and Aromatic Hydrocarbons, in *Ul'trazvuk i fiziko-khimicheskie svoistva veshchestva* (Ultrasound and the Physicochemical Properties of Matter), Kursk: Izd. KGPI (Kursk State Pedagogical Inst.), 1969, p. 63.
56. Pishchikov, I.M., An Investigation of the Velocity and Absorption of Sound in Diphenyl, in *Ul'trazvuk i fiziko-khimicheskie svoistva veshchestva* (Ultrasound and the Physicochemical Properties of Matter), Kursk: Izd. KGPI (Kursk State Pedagogical Inst.), 1969, p. 70.
57. Tutov, V.M., An Investigation of the Temperature Dependence of the Sound Velocity in Some Liquid Hydrocarbons, in *Ul'trazvuk i fiziko-khimicheskie svoistva veshchestva* (Ultrasound and the Physicochemical Properties of Matter), Kursk: Izd. KGPI (Kursk State Pedagogical Inst.), 1969, p. 87.
58. Neruchev, Yu.A., The Sound Velocity and Adiabatic Compressibility of *n*-Paraffins in the Vicinity of the Critical Point, in *Ul'trazvuk i fiziko-khimicheskie svoistva veshchestva* (Ultrasound and the Physicochemical Properties of Matter), Kursk: Izd. KGPI (Kursk State Pedagogical Inst.), 1969, p. 92.
59. Zotov, V.V., Otpushchennikov, N.F., and Neruchev, Yu.A., Experimental Investigation of the Sound Velocity in *n*-Xylene, *o*-Xylene, and *n*-Butyl Benzene on the Saturation Curve, in *Ul'trazvuk i fiziko-khimicheskie svoistva veshchestva* (Ultrasound and the Physicochemical Properties of Matter), Kursk: Izd. KGPI (Kursk State Pedagogical Inst.), 1970, p. 67.
60. Zotov, V.V. and Shoitov, Yu.S., The Sound Velocity in Glycerin, Ethylene Glycol, and Diethylene Glycol, in *Ul'trazvuk i fiziko-khimicheskie svoistva veshchestva* (Ultrasound and the Physicochemical Properties of Matter), Kursk: Izd. KGPI (Kursk State Pedagogical Inst.), 1970, p. 92.
61. Pishchikov, I.M., An Investigation of the Ultrasonic Velocity in Dicumyl Methane, in *Ul'trazvuk i fiziko-khimicheskie svoistva veshchestva* (Ultrasound and the Physicochemical Properties of Matter), Kursk: Izd. KGPI (Kursk State Pedagogical Inst.), 1970, p. 172.
62. Kir'yakov, B.S. and Otpushchennikov, N.F., The Sound Velocity in the *n*-Paraffin Series in the Pressure Range from Zero to 2000 atm, in *Ul'trazvuk i fiziko-khimicheskie svoistva veshchestva* (Ultrasound and the Physicochemical Properties of Matter), Kursk: Izd. KGPI (Kursk State Pedagogical Inst.), 1972, p. 16.
63. Kireev, B.N. and Otpushchennikov, N.F., Experimental Investigation of the Sound Velocity in Some Olefins on the Saturation Curve, in *Ul'trazvuk i fiziko-khimicheskie svoistva veshchestva* (Ultrasound and the Physicochemical Properties of Matter), Kursk: Izd. KGPI (Kursk State Pedagogical Inst.), 1972, p. 47.
64. Korabel'nikov, A.V. and Ivanova, O.P., The Acoustic and Thermodynamic Properties of Some Organic Liquids, in *Ul'trazvuk i fiziko-khimicheskie svoistva veshchestva* (Ultrasound and the Physicochemical Properties of Matter), Kursk: Izd. KGPI (Kursk State Pedagogical Inst.), 1972, p. 63.
65. Korabel'nikov, A.V., Otpushchennikov, N.F., and Ivanova, O.P., The Acoustic and Thermodynamic Properties of Some Monosubstituted Benzene Compounds, in *Ul'trazvuk i fiziko-khimicheskie svoistva veshchestva* (Ultrasound and the Physicochemical Properties of Matter), Kursk: Izd. KGPI (Kursk State Pedagogical Inst.), 1972, p. 89.
66. Zavarykina, L.N. and Kireev, B.N., The Acoustic and Thermodynamic Properties of Pentene-1, in *Ul'trazvuk i fiziko-khimicheskie svoistva veshchestva* (Ultrasound and the Phys-

icochemical Properties of Matter), Kursk: Izd. KGPI (Kursk State Pedagogical Inst.), 1973, p. 71.

67. Korabel'nikov, A.V. and Otpushchennikov, N.F., The Procedure of Measurement of the Ultrasonic Velocity on the Saturation Curve, in *Ul'trazvuk i fiziko-khimicheskie svoistva veshchestva* (Ultrasound and the Physicochemical Properties of Matter), Kursk: Izd. KGPI (Kursk State Pedagogical Inst.), 1973, p. 122.
68. Kireev, B.S. and Melikhov, Yu.F., The Acoustic and Thermodynamic Properties of Octene-1 on the Saturation Curve, in *Ul'trazvuk i fiziko-khimicheskie svoistva veshchestva* (Ultrasound and the Physicochemical Properties of Matter), Kursk: Izd. KGPI (Kursk State Pedagogical Inst.), 1974, p. 35.
69. Kireev, B.S. and Otpushchennikov, N.F., An Investigation of the Elastic Properties of Saturated Ethers and Ketones by the Acoustic Method, in *Ul'trazvuk i fiziko-khimicheskie svoistva veshchestva* (Ultrasound and the Physicochemical Properties of Matter), Kursk: Izd. KGPI (Kursk State Pedagogical Inst.), 1974, p. 80.
70. Korabel'nikov, A.V., The Temperature Dependence of the Ultrasonic Velocity in the Liquid and Vapor Phases of Fluorobenzene on the Saturation Curve, in *Ul'trazvuk i fiziko-khimicheskie svoistva veshchestva* (Ultrasound and the Physicochemical Properties of Matter), Kursk: Izd. KGPI (Kursk State Pedagogical Inst.), 1974, p. 93.
71. Timofeev, N.E. and Otpushchennikov, N.F., The Acoustic and Some Thermodynamic Properties of Carbon Tetrachloride on the Saturation Curve, in *Ul'trazvuk i fiziko-khimicheskie svoistva veshchestva* (Ultrasound and the Physicochemical Properties of Matter), Kursk: Izd. KGPI (Kursk State Pedagogical Inst.), 1975, p. 175.
72. Nikiforov, S.A., An Investigation of the Elastic Properties of Organosilicon Liquids by the Acoustic Method, in *Ul'trazvuk i fiziko-khimicheskie svoistva veshchestva* (Ultrasound and the Physicochemical Properties of Matter), Kursk: Izd. KGPI (Kursk State Pedagogical Inst.), 1975, p. 203.
73. Timofeev, N.E. and Kuz'min, V.N., The Acoustic and Some Thermodynamic Properties of *n*-Tetradecane on the Saturation Curve, in *Ul'trazvuk i fiziko-khimicheskie svoistva veshchestva* (Ultrasound and the Physicochemical Properties of Matter), Kursk: Izd. KGPI (Kursk State Pedagogical Inst.), 1975, p. 255.
74. Timofeev, N.E., Experimental Investigation of the Sound Velocity in Some 1-Alkynes on the Saturation Curve, in *Ul'trazvuk i fiziko-khimicheskie svoistva veshchestva* (Ultrasound and the Physicochemical Properties of Matter), Kursk: Izd. KGPI (Kursk State Pedagogical Inst.), 1977, p. 88.
75. Timofeev, N.E. and Otpushchennikov, N.F., An Investigation of the Elastic Properties of Some Higher *n*-Alcohols on the Liquid–Vapor Equilibrium Line, in *Ul'trazvuk i fiziko-khimicheskie svoistva veshchestva* (Ultrasound and the Physicochemical Properties of Matter), Kursk: Izd. KGPI (Kursk State Pedagogical Inst.), 1977, p. 165.
76. Timofeev, N.E., The Sound Velocity and Adiabatic Compressibility in Higher *n*-Alcohols on the Saturation Curve, in *Ul'trazvuk i fiziko-khimicheskie svoistva veshchestva* (Ultrasound and the Physicochemical Properties of Matter), Kursk: Izd. KGPI (Kursk State Pedagogical Inst.), 1977, p. 97.
77. Timofeev, N.E., Experimental Investigations of the Ultrasonic Velocity in Vapors of Hydrocarbons of the Acetylene Series, in *Ul'trazvuk i fiziko-khimicheskie svoistva veshchestva* (Ultrasound and the Physicochemical Properties of Matter), Kursk: Izd. KGPI (Kursk State Pedagogical Inst.), 1978, p. 110.
78. Korabel'nikov, A.V., The Acoustic Properties of Dioxan on the Saturation Curve, in *Ul'trazvuk i fiziko-khimicheskie svoistva veshchestva* (Ultrasound and the Physicochemical Properties of Matter), Kursk: Izd. KGPI (Kursk State Pedagogical Inst.), 1978, p. 118.
79. Timofeev, N.E. and Nikolaev, S.N., The Molecular Structure of Cycloparaffins and the Temperature Dependence of the Sound Velocity in Them on the Saturation Curve, in *Ul'trazvuk i termodinamicheskie svoistva veshchestva* (Ultrasound and the Thermodynamic Properties of Matter), Kursk: Izd. KGPI (Kursk State Pedagogical Inst.), 1982, p. 81.
80. Tsydypov, Sh.B. and Otpushchennikov, N.F., The Acoustic and Thermodynamic Properties of Diphenyl Carbon Tetrachloride on the Liquid–Vapor Equilibrium Line, in *Ul'trazvuk i termodinamicheskie svoistva veshchestva* (Ultrasound and the Thermodynamic Properties of Matter), Kursk: Izd. KGPI (Kursk State Pedagogical Inst.), 1982, p. 98.
81. Pevnyi, E.M., Results of Experimental Investigation of the Velocity of Propagation of Ultrasound in Diallyl Oxide, in *Ul'trazvuk i termodinamicheskie svoistva veshchestva* (Ultrasound and the Thermodynamic Properties of Matter), Kursk: Izd. KGPI (Kursk State Pedagogical Inst.), 1983, p. 59.
82. Timofeev, N.E. and Alekseev, V.V., The Sound Velocity and Some Thermodynamic Properties of *n*- and Iso-Propyl Alcohols on the Saturation Curve at Low Temperatures, in *Ul'trazvuk i termodinamicheskie svoistva veshchestva* (Ultrasound and the Thermodynamic Properties of Matter), Kursk: Izd. KGPI (Kursk State Pedagogical Inst.), 1983, p. 142.
83. Tsydypov, Sh.B. and Otpushchennikov, N.F., Experimental Investigation of the Velocity of Propagation of Ultrasound in Some Aromatic Hydrocarbons on the Saturation Curve, in *Ul'trazvuk i termodinamicheskie svoistva veshchestva* (Ultrasound and the Thermodynamic Properties of Matter), Kursk: Izd. KGPI (Kursk State Pedagogical Inst.), 1984, p. 166.
84. Verveiko, V.N. and Mel'nikov, G.A., An Investigation of Aromatic Hydrocarbons and Their Halogenated Compounds by the Acoustic Piezometer Technique at High Pressures, in *Ul'trazvuk i termodinamicheskie svoistva veshchestva* (Ultrasound and the Thermodynamic Properties of Matter), Kursk: Izd. KGPI (Kursk State Pedagogical Inst.), 1989, p. 30.
85. Melent'ev, V.V. and Neruchev, Yu.A., An Investigation of the Acoustic Properties of Some *n*-Paraffins and Their Chloro-Compounds, in *Ul'trazvuk i termodinamicheskie svoistva veshchestva* (Ultrasound and the Thermodynamic Properties of Matter), Kursk: Izd. KGPI (Kursk State Pedagogical Inst.), 1990, p. 129.
86. Shakhov, A.V., Mel'nikov, G.A., Neruchev, Yu.A., and Parfir'ev, V.B., The Elastic and Caloric Properties of Halogenated Alkyl Benzenes, in *Ul'trazvuk i termodinamicheskie*

svoistva veshchestva (Ultrasound and the Thermodynamic Properties of Matter), Kursk: Izd. KGPI (Kursk State Pedagogical Inst.), 1993, p. 50.

87. Melent’ev, V.V., The density and Elastic Properties of *n*-hexane, *n*-heptane, and Their Chloro- and Iodine Compounds, in *Ul’trazvuk i termodinamicheskie svoistva veshchestva* (Ultrasound and the Thermodynamic Properties of Matter), Kursk: Izd. KGPI (Kursk State Pedagogical Inst.), 1993, p. 63.
88. Shakhov, A.V., Mel’nikov, G.A., and Davydova, N.V., The Thermal Properties of Halogenated Compounds of Toluene on the Saturation Curve, in *Ul’trazvuk i termodinamicheskie svoistva veshchestva* (Ultrasound and the Thermodynamic Properties of Matter), Kursk: Izd. KGPI (Kursk State Pedagogical Inst.), 1994, p. 42.
89. Shakhov, A.V., Mel’nikov, G.A., and Davydova, N.V., The Structure and Thermodynamic Properties of *o*-Fluorochlorobenzene, in *Ul’trazvuk i termodinamicheskie svoistva veshchestva* (Ultrasound and the Thermodynamic Properties of Matter), Kursk: Izd. KGPU (Kursk State Pedagogical Univ.), 1997, p. 38.
90. Shakhov, A.V. and Mel’nikov, G.A., The Elastic Properties of Fluorobenzotrichloride, in *Ul’trazvuk i termodinamicheskie svoistva veshchestva* (Ultrasound and the Thermodynamic Properties of Matter), Kursk: Izd. KGPU (Kursk State Pedagogical Univ.), 1998, p. 63.
91. Shakhov, A.V. and Neruchev, Yu.A., *J. Eng. Thermophys*, 2003, vol. 11, no. 4, p. 335.
92. Bolotnikov, M. and Neruchev, Yu., *J. Chem. Eng. Data*, 2003, vol. 48, p. 411.
93. Skryshevskii, A.F., *Strukturnyi analiz zhidkostei i amorfnykh tel* (Structure Analysis of Liquids and Amorphous Bodies), Moscow: Vysshaya Shkola, 1980.
94. Mel’nikov, G.A., Skryshevskii, A.F., and Otpushchennikov, N.F., *Fiz. Zhidk. Sostoyaniya*, 1986, issue 14, p. 68.
95. Kitaigorodskii, A.I., *Molekulyarnye kristally* (Molecular Crystals), Moscow: Nauka, 1971.
96. Vol’kenshtein, M.V., Emel’yashevich, M.Ya., and Stepanov, I.V., *Kolebaniya molekul* (Molecular Vibrations), Moscow: Gostekhizdat, 1949, vols. 1 and 2.
97. Vol’kenshtein, M.V., *Stroyenie i fizicheskie svoistva molekul* (The Structure and Physical Properties of Molecules), Moscow: Izd. AN SSSR (USSR Acad. Sci.), 1955.
98. Chavez, M., Palaclos, J.M., and Tsumura, R., *J. Chem. Eng. Data*, 1992, vol. 27, p. 350.
99. Golik, A.Z. and Adamenko, I.I., in *Teplofizicheskie svoistva zhidkostei* (Thermophysical Properties of Liquids), Moscow: Nauka, 1976, p. 5.
100. Garkusha, L.I., The Mechanism of Thermal Motion in Some Hydrocarbons and Their Mutual Solutions, *Cand. Sci. (Phys.-Math.) Dissertation*, Kiev: Kiev State Univ., 1990.
101. Freyer, E.B., Hubbard, J.C., and Andrews, D.N., *J. Am. Chem. Soc.*, 1929, vol. 51, p. 759.
102. Kuzovkov, Yu.I. and Tarasenko, O.V., An Investigation of the temperature dependence of Adiabatic Compressibility and Bulk Viscosity of *n*-Paraffins on the Liquid-Vapor Equilibrium Line, in *Ul’trazvuk i fiziko-khimicheskie svoistva veshchestva* (Ultrasound and the Physicochemical Properties of Matter), Kursk: Izd. KGPI (Kursk State Pedagogical Inst.), 1974, p. 206.
103. Neruchev, Yu.A., The Calculation of Critical Temperature and Sound Velocity of *n*-alkanes on the Saturation Curve, in *Ul’trazvuk i fiziko-khimicheskie svoistva veshchestva* (Ultrasound and the Physicochemical Properties of Matter), Kursk: Izd. KGPI (Kursk State Pedagogical Inst.), 1970, p. 34.
104. Neruchev, Yu.A. and Zotov, V.V., The Recommended Values of Some Thermodynamic Properties of *n*-Paraffins on the Saturation Curve, in *Ul’trazvuk i fiziko-khimicheskie svoistva veshchestva* (Ultrasound and the Physicochemical Properties of Matter), Kursk: Izd. KGPI (Kursk State Pedagogical Inst.), 1977, p. 7.
105. Mel’nikov, G.A., Verveiko, V.N., and Otpushchennikov, N.F., *Zh. Fiz. Khim.*, 1988, vol. 62, no. 3, p. 798.
106. Levin, V.V., *Fiz. Fiz. Khim. Zhidk.*, 1972, issue 1, p. 176.
107. *Vrednye khimicheskie veshchestva. Uglevodorody. Galogenproizvodnye uglevodorodov: Spravochnoe izdanie* (Harmful Chemical Substances. Hydrocarbons. Halogen Derivatives of Hydrocarbons: A Reference Book), Filov, V.A. *et al.*, Eds., Leningrad: Khimiya, 1990.
108. Melent’ev, V.V., Integrated Studies of the Thermal Properties of *n*-alkanes and Their Halogenated Compounds, *Cand. Sci. (Phys.-Math.) Dissertation*, Kursk: Kursk State Technical Univ., 1997.
109. Bolotnikov, M.F., Investigation of Excess Properties of Binary Mixtures of Liquids of Paraffin Series Based on Acoustic and Caloric Measurements, *Cand. Sci. (Phys.-Math.) Dissertation*, Kursk: Kursk State Technical Univ., 1999.
110. Skryshevskii, A.F. and Mamedov, K.P., in *Voprosy fiziki metallov i metallovedeniya* (Problems in the Physics of Metals and Metal Studies), Kiev: AN USSR (Acad. Sci. of Ukrainian SSR), 1954, no. 5.
111. Shustorovich, E.M., *Priroda khimicheskoi svyazi* (The Nature of Chemical Bond), Moscow: Izd. AN SSSR (USSR Acad. Sci.), 1963.
112. Katzoff, S., *J. Chem. Phys.*, 1934, vol. 2, p. 841.
113. Okhotin, V.S., Razumeichenko, L.A., and Skorodumov, A.V., The Sound Velocity in Liquid Toluene at Atmospheric Pressure, in *Ul’trazvuk i termodinamicheskie svoistva veshchestva* (Ultrasound and the Thermodynamic Properties of Matter), Kursk: Izd. KGPI (Kursk State Pedagogical Inst.), 1986, p. 106.
114. Okhotin, V.S., Razumeichenko, L.A., Kas’yanov, Yu.I. *et al.*, The Sound Velocity in Liquid *m*-Xylene, in *Termodinamika i teplofizicheskie svoistva veshchestva* (The Thermodynamics and Thermal Properties of Matter), Moscow: MEI (Moscow Inst. of Power Engineering), 1987, no. 131, p. 42.
115. Okhotin, V.S., Razumeichenko, L.A., Kas’yanov, Yu.I. *et al.*, An Experimental Investigation of the Sound Velocity and Heat Capacity of Liquid *m*-Xylene, in *Ul’trazvuk i termodinamicheskie svoistva veshchestva* (Ultrasound and the Thermodynamic Properties of Matter), Kursk: Izd. KGPI (Kursk State Pedagogical Inst.), 1986, p. 106.
116. Makhno, M.G., Studies of the Equation of State and Equilibrium Properties of Molecular Liquids, *Cand. Sci. (Phys.-Math.) Dissertation*, Kiev: Kiev State Univ., 1983.

117. Shakhov, A.V., Investigation of the Thermal Properties of Benzene and Its Derivatives, *Cand. Sci. (Phys.-Math.) Dissertation*, Kursk: Kursk State Univ., 2003.

118. Evans, R.C., *An Introduction to Crystal Chemistry*, Cambridge: Cambridge University Press, 1939. Translated under the title *Vvedenie v kristallokhimiyu*, Moscow: Goskhimizdat, 1948.

119. Skryshevskii, A.F., *Rentgenografiya zhidkostei* (X-Ray Radiography of Liquids), Kiev: Kiev State Univ., 1956.

120. Khasanshin, T.S., *Teplofizicheskie svoistva predel'nykh odnoatomnykh spirtov pri atmosfernom davlenii* (The Thermal Properties of Saturated Monatomic Alcohols at Atmospheric Pressure), Minsk: Izd. Standartov, 1992.

121. Novikov, I.I., *Teplofiz. Vys. Temp.*, 2001, vol. 39, no. 1, p. 47 (*High Temp.* (Engl. transl.), vol. 39, no. 1, p. 43).

122. Novikov, I.I., *Teplofiz. Vys. Temp.*, 2003, vol. 41, no. 4, p. 511 (*High Temp.* (Engl. transl.), vol. 41, no. 4, p. 443).

123. Shimanskaya, E.T., Shimanskii, Yu.I., and Golik, A.Z., in *Kriticheskie yavleniya i flyuktuatsii v rastvorakh* (Critical Phenomena and Fluctuations in Solutions), Moscow: AN SSSR (USSR Acad. Sci.), 1960.

124. *Uravneniya sostoyaniya gazov i zhidkostei* (Equations of State for Gases and Liquids), Novikov, I.I., Ed., Moscow: Nauka, 1975.

125. Fisher, M., *The Nature of Critical Points*, Boulder: University of Colorado Press, 1965. Translated under the title *Priroda kriticheskogo sostoyaniya*, Moscow: Mir, 1968.

126. Grigor'ev, B.A., Rastorguev, Yu.L., Gerasimov, A.A., Kurumov, D.S., and Plotnikov, S.A., *Termodinamicheskie svoistva normal'nogo geksana* (The Thermodynamic Properties of Normal Hexane), Moscow: Izd. Standartov, 1990.

127. Vargaftik, N.B., *Spravochnik po teplofizicheskim svoistvam gazov i zhidkostei*, Moscow: Nauka, 1972.Translated under the title *Tables of the Thermophysical Properties of Liquids and Gases*, New York: Halsted Press, 1975.

128. Amirkhanov, Kh.I., Alibekov, B.G., Vikhrov, D.I., and Mirskaya, V.A., *Izokhornaya teploemkost' i drugie kaloricheskie svoistva uglevodorodov metanovogo ryada* (Isochoric Heat Capacity and Other Caloric Properties of Hydrocarbons of the Methane Series), Makhachkala: Dagestanskoe Knizhnoe Izd., 1981.

129. Zotov, V.V. and Neruchev, Yu.A., The Elastic and Caloric Properties of *n*-hexane on the Liquid-Vapor Equilibrium Curve, in *Ul'trazvuk i termodinamicheskie svoistva veshchestva* (Ultrasound and the Thermodynamic Properties of Matter), Kursk: Izd. KGPI (Kursk State Pedagogical Inst.), 1986, p. 34.

130. Tatevskii, V.M., *Fiziko-khimicheskie svoistva individual'nykh uglevodorodov* (The Physicochemical Properties of Individual Hydrocarbons), Moscow: Gostoptekhizdat, 1960.

131. Eduljee, H.E., Newitt, D.M., and Weale, K.T., *J. Chem. Soc.*, 1951, vol. 3, no. 4, p. 2086.

132. Gallant, L.W., *Hydrocarbon Process.*, 1967, vol. 46, no. 7, p. 121.

133. Taplin, N.S. and Zusic, D.A., *Hydrocarbon Process.*, 1967, vol. 46, no. 8, p. 145.

134. Landau, L.D. and Lifshitz, E.M., *Statisticheskaya fizika* (Statistical Physics), Moscow: Nauka, 1964.

135. Filippov, L.P., *Podobie svoistv veshchestva* (The Similarity of Properties of Matter), Moscow: MGU (Moscow State Univ.), 1978.

136. Filippov, L.P., *Zakon sootvetstvennykh sostoyanii* (The Law of Corresponding States), Moscow: MGU (Moscow State Univ.), 1983.

137. Boelhouwer, J.W.M., *Physics*, 1960, vol. 26, p. 1021.

138. Doolittle, A.K., *Chem. Eng. Prog.*, 1970, vol. 59, no. 44, p. 1.

139. Neruchev, Yu.A., *Diskretno-kontinual'naya model' dlya prognozirovaniya ravnovesnykh svoistv organicheskikh zhidkostei* (A Discrete-Continual Model for Prediction of the Equilibrium Properties of Organic Liquids), Kursk: Izd. KGPU (Kursk State Pedagogical Univ.), 2001.